Development 140, 3787-3798 (2013) doi:10.1242/dev.093567

Tmem88a mediates GATA-dependent specification of cardiomyocyte progenitors by restricting WNT signaling

Natasha Novikov and Todd Evans*

SUMMARY

Biphasic control of WNT signaling is essential during cardiogenesis, but how the pathway switches from promoting cardiac mesoderm to restricting cardiomyocyte progenitor fate is unknown. We identified genes expressed in lateral mesoderm that are dysregulated in zebrafish when both *gata5* and *gata6* are depleted, causing a block to cardiomyocyte specification. This screen identified *tmem88a*, which is expressed in the early cardiac progenitor field and was previously implicated in WNT modulation by overexpression studies. Depletion of *tmem88a* results in a profound cardiomyopathy, secondary to impaired cardiomyocyte specification. In *tmem88a* morphants, activation of the WNT pathway exacerbates the cardiomyocyte deficiency, whereas WNT inhibition rescues progenitor cells and cardiogenesis. We conclude that specification of cardiac fate downstream of *gata5/6* involves activation of the *tmem88a* gene to constrain WNT signaling and expand the number of cardiac progenitors. Tmem88a is a novel component of the regulatory mechanism controlling the second phase of biphasic WNT activity essential for embryonic cardiogenesis.

KEY WORDS: Zebrafish, Heart development, Lineage commitment, Cardiac fate

INTRODUCTION

Heart formation is a dynamic process involving cardiomyocyte progenitor (CP) specification, cell migration, cardiomyocyte differentiation and complex tissue morphogenesis (Brand, 2003; Evans et al., 2010; Harvey, 2002). Retrospective clonal lineage analysis has identified at least two major CP populations that contribute to the heart (Buckingham et al., 2005; Meilhac et al., 2004). The first wave of CPs comprises the first heart field (FHF) and differentiates into cardiomyocytes that form the left ventricle, atrioventricular canal and the atria. The second pool of CPs, or the second heart field (SHF), constitutes a highly proliferative cell population that contributes to the right ventricle and outflow tract (Black, 2007; Cai et al., 2003; Kelly et al., 2001; Mjaatvedt et al., 2001; Vincent and Buckingham, 2010; Waldo et al., 2001; Zaffran et al., 2004). The formation of the FHF and SHF and the regulatory network that coordinates CP specification is conserved in human, mouse, chick and zebrafish (Brand, 2003; Liu and Foley, 2011; Zhou et al., 2011). Therefore, molecular insight gleaned from model systems is relevant to the development of emerging targeted strategies to expand human CPs for therapeutic purposes.

The molecular drivers of CP specification include several well-studied transcription factor families and signaling pathways (Evans et al., 2010; Stainier, 2001). The generation of precardiac mesoderm requires the function of transcription factors MESP1 and MESP2. In chimeric mouse embryos, cells doubly mutant for *Mesp1* and *Mesp2* selectively fail to contribute to the heart (Saga et al., 2000). Downstream transcription factors believed to impact CP specification belong to the GATA, NK2, MEF2, SRF, ISL and TBX families. Various combinations of these factors selectively influence FHF or SHF development (Buckingham et al., 2005; Meilhac et al., 2004). Cooperating signaling molecules that enhance CP expansion include those from the BMP, FGF, HH, Nodal, retinoid and WNT families. BMPs and FGFs are secreted by cardiac-associated endoderm (Foley et al., 2006; Lough and Sugi, 2000), whereas HH and Nodal act cell-autonomously to stimulate specification (Keegan et al., 2004; Thomas et al., 2008). By contrast, retinoic acid (RA) inhibits CPs. RA delineates the forelimb organ field and induces *Hox5b* expression, which prevents caudal CP expansion into the neighboring forelimb territory (Waxman et al., 2008). RA also increases levels of the LIM protein Ajuba, which limits SHF formation by repressing the SHF-specific transcription factor *Islet1* (Witzel et al., 2012). Rostrally, the domain of CP specification is limited by neighboring vascular and hematopoietic tissue. Hematovascular transcription factors SCL and ETSRP can override CP fate (Schoenebeck et al., 2007).

Understanding the function of the WNT pathway for CP specification has been more challenging, as canonical WNT signaling both promotes and restrains CP specification (Kwon et al., 2007; Lavery et al., 2008; Naito et al., 2006; Paige et al., 2010; Tzahor, 2007; Ueno et al., 2007). During gastrulation, WNT activity induces ventrolateral mesoderm to establish the precardiac territory. Subsequently, WNT signaling restricts CP specification. Other than being cell-autonomous, the molecular mechanism of WNT-mediated inhibition of specification is undefined. However, ectopic WNT activation correlates with reduced GATA factor expression (Afouda et al., 2008; Martin et al., 2010).

GATA factors are zinc-finger transcriptional regulators that control organ development (Patient and McGhee, 2002). *Gata4*, *Gata5* and *Gata6* each contribute to numerous aspects of vertebrate cardiogenesis. We showed previously that *gata5* and *gata6* function together as essential components for CP specification in zebrafish (Holtzinger and Evans, 2007). When both factors are simultaneously depleted, there is a complete failure in the formation of *nkx2.5*$^{+}$ CPs, and the corresponding embryos develop without hearts. Loss-of-function studies in other species, including ascidians (Ragkousi et al., 2011), flies (Klinedinst and Bodmer, 2003) and mice (Singh et al., 2010; Zhao et al., 2008), confirm the requirement of GATA factors for cardiogenesis and, in particular, CP specification.

Department of Surgery, Weill Cornell Medical College, Cornell University, 1300 York Ave., LC-708, New York, NY, USA.

*Author for correspondence (tre2003@med.cornell.edu)

Accepted 1 July 2013

Gain-of-function experiments have shown that GATA factors can integrate into molecular complexes sufficient for specification (Ieda et al., 2010; Lou et al., 2011; Takeuchi and Bruneau, 2009). For example, combined expression of *Gata4*, *Mef2c* and *Tbx5* in postnatal mouse fibroblasts was reported to reprogram fibroblasts into cardiomyocytes (Ieda et al., 2010). In embryonic mouse explants, ectopic expression of *Gata4* and *Baf60c* (*Smarcd3*), which encodes a chromatin-remodeling protein, conferred cardiogenic fate onto non-cardiogenic mesoderm (Takeuchi and Bruneau, 2009). Cell transplantation studies in zebrafish further demonstrated that GATA factors and Baf60c (Smarcd3b) act cell-autonomously to impact cardiac fate (Lou et al., 2011).

Despite their importance, the mechanism by which GATA factors impact CP specification is unknown. Cardiac transcription factors, including GATA factors, cross-regulate each other at both the transcriptional and post-transcriptional levels (Zhou et al., 2012), but it is less clear how they integrate into the established signaling network that modulates CP specification. Here, we take advantage of the zebrafish model, which is dependent on *gata5* and *gata6* for CP formation, to screen for downstream transcriptional targets potentially involved in cardiac specification. One of the top candidates to emerge from this screen is *tmem88a*, which encodes a transmembrane protein and putative negative regulator of canonical WNT signaling. We show that GATA factors act through *tmem88a* to modulate WNT signaling and thereby regulate CP specification.

MATERIALS AND METHODS

Zebrafish strains and maintenance

Embryos were raised at 28.5°C and morphologically staged as described (Kimmel et al., 1995). All experimental procedures were conducted in compliance with the Weill Cornell Medical College IACUC. Wild-type embryos were derived from crosses of the AB and TU lines. The following strains were used: *tp53*^{M214K} (Berghmans et al., 2005), *cloche* (Stainier et al., 1995), *tg(myl7:eGFP)* (Huang et al., 2003), *tg(myl7:dsRed2-nuc)* (Mably et al., 2003), *tg(hsp70l:dkk1-eGFP)* (Stoick-Cooper et al., 2007), *tg(hsp70l:wnt8a-eGFP)* (Weidinger et al., 2005) and *TOPdGFP* (Dorsky et al., 2002).

Morpholinos (MOs)

Translation-blocking (5′-GGAAGACTCATCTTGCCGTTCATCA) and splice-blocking (5′-TGACGCTGAACCTGTGGAACACAGA) MOs were used to target *tmem88a* (Gene Tools) at optimal doses of 6 ng and 8 ng, respectively. All experiments, apart from MO validation, were performed using the translation blocker. Standard control MO (5′-CCTCTTACCTCAGTTACAATTTATA) and previously described *gata5* and *gata6* MOs were also used (Holtzinger and Evans, 2007).

Capped mRNA

The *tmem88a* cDNA was PCR amplified and cloned into the pCS2+ vector (D. Turner, U. Michigan). A mutant *tmem88a* construct was also generated containing a frameshift mutation predicted to cause protein truncation. Capped mRNA was synthesized *in vitro* (mMESSAGE mMACHINE, Invitrogen), diluted in RNase-free water and microinjected at 200 pg.

RNA sequencing

Samples prepared with the Illumina mRNA-seq Sample Preparation Kit were sequenced on the Illumina Genome Analyzer IIx with single 36 bp reads. Alignment to the zebrafish Zv9.61 genome was performed with the Burrows-Wheeler Aligner (Li and Durbin, 2009). Differential expression analysis was conducted in DESeq/Bioconductor R (Anders and Huber, 2010) with DESeq adjusted $P<0.05$, RPKM >1.00 and fold-change >2.00. Biological significance was inferred by gene ontology annotation through the Database for Annotation, Visualization and Integrated Discovery (DAVID) (Huang et al., 2009a; Huang et al., 2009b). Analysis was facilitated by GobyWeb (Dorff et al., 2012). The raw data are available at Gene Expression Omnibus (http://www.ncbi.nlm.nih.gov/projects/geo/) with accession number GSE44026.

Whole-mount *in situ* hybridization (WISH)

WISH was performed as described (Jowett, 1998). The *tmem88a* sequence was PCR amplified from cDNA clone MDR1734-9140265 (OpenBiosystems) using forward primer 5′-GAGTAGAGCAGG-AAAGAAGGAAGA and reverse primer 5′-GAATTTTAAACAG-GGGTTTATCCA and ligated into the pCS2+ vector. The riboprobe was synthesized from an *Eco*RI-linearized plasmid with T7 RNA polymerase. Additional probes were prepared as described previously: *nkx2.5*, *myl7*, *amhc*, *vmhc* (Reiter et al., 1999); *scl*, *gata1* (Liao et al., 1998); *gata4* (Heicklen-Klein and Evans, 2004); *ntl* (Schulte-Merker et al., 1992); *pax2a* (Krauss et al., 1991); and *myod* (Weinberg et al., 1996). Tyramide signal amplification (TSA) dual fluorescent *in situ* hybridization was performed as described (Brend and Holley, 2009). A fluorescein-labeled *tmem88a* probe and a digoxigenin-labeled mixture of *nkx2.5* and *ntl* probes were hybridized overnight at 65°C. The TSA Plus Cyanine 5/Fluorescein System (Perkin Elmer) was used to develop the riboprobe signals.

Cell death and proliferation assays

TSA fluorescent *in situ* hybridization for digoxigenin-labeled *nkx2.5* and *ntl* probes was combined with TMR-Red *In Situ* Cell Death Detection (Roche) or phospho-Histone H3 (PH3) immunohistochemistry (Millipore). For TSA/PH3 staining, embryos were fixed for 2 hours in 4% paraformaldehyde and riboprobe hybridization was performed at 55°C. The primary anti-PH3 antibody was diluted 1:200 dilution and detected with goat anti-rabbit IgG Alexa 546 (Invitrogen) diluted 1:500.

RNA isolation and quantitative RT-PCR

RNA isolated using Trizol Reagent (Invitrogen) was reverse transcribed with the Superscript III First-Strand Synthesis System (Invitrogen). The *tmem88a* transcript was detected with forward primer 5′-TCATCTTTGGCCTCATCCTC-3′ and reverse primer 5′-AAAGCAACACAGCCTCCATC-3′. Gene expression was normalized to *β-actin* levels (Holtzinger and Evans, 2007). Relative fold change was determined as described (Livak and Schmittgen, 2001).

Immunohistochemistry

Immunohistochemistry on zebrafish hearts was performed as described (Yang and Xu, 2012). Anti-DsRed2 (Clontech) was diluted 1:100 and detected with goat anti-rabbit IgG Alexa 546 (Invitrogen). S46 (DSHB) was diluted 1:20 and detected with goat anti-mouse IgG1 Alexa 647 (Invitrogen). Secondary antibodies were diluted 1:500.

Image acquisition and analysis

Live embryos were imaged using a Nikon SMZ1500 with an Insight Firewire 2 digital camera and SPOT advanced imaging software. WISH preparations were mounted in glycerol and similarly imaged. TSA-treated embryos and embryonic hearts were imaged using the Zeiss LSM 510 confocal microscope with Zen software. The 40× and 20× objectives were used, respectively. Images were analyzed in ImageJ (NIH) and Adobe Photoshop. Student's *t*-test was used to assess statistical significance. All data were graphed with error bars corresponding to one standard deviation of the mean.

Heat-shock experiments

Embryos were heat shocked at 39°C and subsequently screened for *eGFP* expression to confirm the presence of the transgenic allele in either *tg(hsp70l:dkk1-eGFP)* or *tg(hsp70l:wnt8a-eGFP)* background.

RESULTS

Identification of genes regulated cooperatively by *gata5/6* and associated with CP specification during embryogenesis

Gata5 and Gata6 independently regulate heart morphogenesis, but together they act to coordinate CP specification (Holtzinger and Evans, 2007). Based on this observation, we developed a strategy to

identify *gata5* and *gata6* (*gata5/6*) co-dependent candidate genes involved in CP specification. A next-generation sequencing screen was performed comparing RNA samples from *gata5/6* double-morphant embryos with wild-type controls and individual *gata5* or *gata6* morphants. Transcription profiles were evaluated to identify genes uniquely dysregulated in *gata5/6* double morphants (Fig. 1A). Samples were collected at the bud or 6-somite stage of development. Bud stage corresponds to the end of gastrulation and onset of precardiac patterning in the lateral mesoderm. At the 6-somite stage, the expression pattern of the CP marker *nkx2.5* has previously been used to reliably assess CP formation (Chen and Fishman, 1996; Hami et al., 2011; Schoenebeck et al., 2007). In wild-type embryos, the expression of *nkx2.5* initiates between the bud and 6-somite stages of development, whereas in *gata5/6* morphants CP specification fails at this time (Fig. 1B). The screen was therefore designed to identify transcriptional components closely associated with the loss of both Gata5 and Gata6 at the time when CP specification fails. The screen does not distinguish between direct or indirect GATA targets.

Using defined criteria, we identified 225 upregulated and 304 downregulated genes specific to the *gata5/6* double morphants (fold change >2; $\Delta gata5/6 > \Delta gata5 + \Delta gata6$; $P<0.05$) (Fig. 1C; supplementary material Table S1). Upregulated genes included a subset of parvalbumins, vitellogenins and serpins. Downregulated genes were mainly associated with hematovascular and cardiac development. In particular, the known CP markers *nkx2.5*, *tbx20* and *gata4* were identified by the screen (Fig. 1D), validating the experimental strategy.

To select genes for further study, we focused on candidates that are expressed in the precardiac mesoderm during embryogenesis. The published whole-mount *in situ* hybridization (WISH) data in the Zebrafish Model Organism Database (ZFIN) was used as a reference to select these candidates (Sprague et al., 2006; Sprague et al., 2008). From the initial set of downregulated genes, 12 were identified (Table 1) as expressed in, or near, the anterior lateral plate mesoderm (ALPM), including *tmem88a*, a gene that encodes a putative transmembrane protein of unknown function.

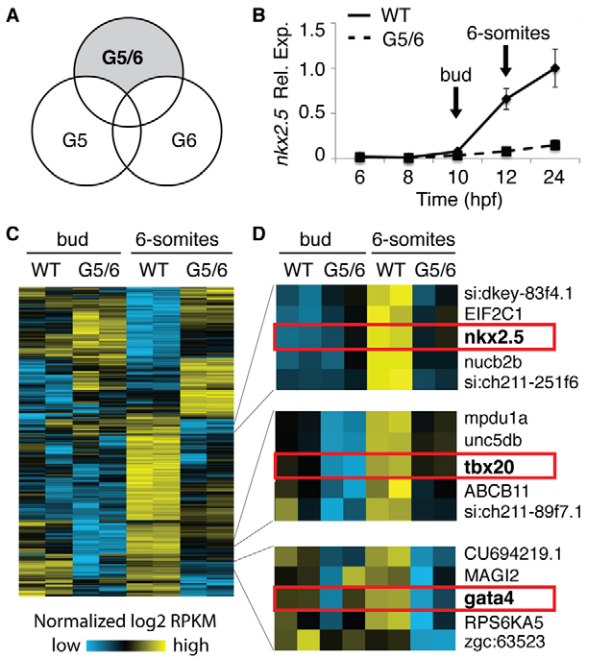

Fig. 1. RNA sequencing screen identifies *gata5/6*-dependent candidate genes involved in CP specification. (**A**) Differential expression analysis of *gata5* (G5), *gata6* (G6) and *gata5/6* (G5/6) morphants, compared with wild-type zebrafish embryos, was used to identify genes preferentially upregulated or downregulated in the G5/6 morphants (gray). (**B**) Relative expression level (Rel. Exp.) of the cardiomyocyte progenitor (CP) marker *nkx2.5* in wild-type (WT) and G5/6 embryos between 6 and 10 hpf, normalized to wild-type expression at 24 hpf. Expression levels of this marker were used to monitor the progress of CP specification. (**C**) Heatmap representation of genes upregulated or downregulated in G5/6 morphants. Expression levels were measured using normalized $\log_2$ reads per kilobase per million mapped reads (RPKM). (**D**) Expanded views of heatmap clusters showing downregulation of known cardiac genes (red boxes) in G5/6 morphants compared with wild type.

Gata5 and Gata6 regulate the expression of *tmem88a* in the ALPM

A role for *tmem88a* in cardiac development has not been described. However, gain-of-function experiments have implicated the human homolog, TMEM88, in the negative regulation of canonical WNT signaling (Lee et al., 2010). Nuclear magnetic resonance and *Xenopus* explant experiments showed that TMEM88 can bind and regulate disheveled 1 (Dvl1), a key player in the WNT pathway. Binding occurs between a highly conserved TMEM88 C-terminal Val-Trp-Val motif and the Dvl1 PDZ domain. Since WNT signaling is an essential mediator of CP specification, we hypothesized that *tmem88a*, co-regulated by Gata5 and Gata6, might potentiate CP specification by modulating WNT activity during embryonic cardiogenesis.

Based on our screen, *tmem88a* is expressed at both the bud and 6-somite stages of development in wild-type zebrafish embryos (Fig. 2A). In *gata5/6* morphants, *tmem88a* expression levels at the bud and 6-somite stages are reduced by ~70% and ~45%, respectively. Using quantitative reverse-transcription PCR (qPCR), we confirmed that *tmem88a* expression is reduced in double morphants, compared with controls, by ~50% (Fig. 2B). WISH analysis of *tmem88a* transcript localization in *gata5/6* morphants and wild-type controls confirmed the *gata5/6* dependency of *tmem88a* expression, particularly within the ALPM (Fig. 2C,D). The *gata5/6*-dependent expression pattern of *tmem88a* implicates a role for this gene in the regulation of lateral mesoderm development.

Table 1. Downregulated genes identified in the *gata5/6* screen that are expressed in or near the APLM

		Fold change	
Ensembl ID	Gene	Bud	6 somites
ENSDARG00000015686	*bmp6*	11.33	3.89
ENSDARG00000005150	*tbx20*	10.80	3.79
ENSDARG00000070542	*mafbb*	7.48	4.48
ENSDARG00000056920	*tmem88a*	3.50	1.49
ENSDARG00000045930	*rbpms2a*	2.87	2.78
ENSDARG00000018004	*nkx2.5*	N.E.	8.06
ENSDARG00000054274	*pcdh10a*	N.E.	2.95
ENSDARG00000045930	*rbpms2b*	N.E.	2.43
ENSDARG00000029764	*mef2ca*	N.E.	2.30
ENSDARG00000059774	*dub*	N.E.	2.23
ENSDARG00000005476	*nav3*	N.E.	2.11
ENSDARG00000035759	*gata4*	N.E.	2.02

N.E., not expressed.

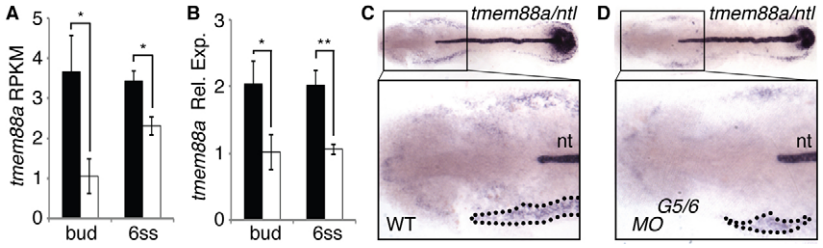

Fig. 2. Confirmation of *gata5/6*-dependent *tmem88a* expression in the anterior lateral plate mesoderm. (**A**,**B**) RNA sequencing *tmem88a* expression in RPKM (A) and qPCR *tmem88a* relative expression (B) for wild-type (black) and *gata5/6* morphants (white) at bud and 6-somite (6ss) stages of development. (**C**,**D**) Transcript localization of *tmem88a* and the regional notochord (nt) marker *ntl*, shown in flatmount *in situ* hybridization preparations of 6-somite stage control (C) and *gata5/6* (D) morphants (dorsal views, anterior to the left). Insets are higher magnifications of the boxed regions. *tmem88a* expression in the anterior lateral plate mesoderm is outlined (dotted line). *n*>20 embryos analyzed per panel. **P*<0.05, ***P*<0.01; error bars indicate s.d.

Expression of *tmem88a* in cardiac progenitors suggests an early role in cardiogenesis

To evaluate the role of Tmem88a in development, the *tmem88a* expression pattern was analyzed in wild-type embryos between the 8-somite stage and 24 hours post-fertilization (hpf), relative to defined markers. At the 8- and 14-somite stages, *tmem88a* transcripts were identified throughout the lateral plate mesoderm (Fig. 3A-D). Notably, *tmem88a* transcripts formed a distinctive 'flare' pattern in the ALPM that was reminiscent of *nkx2.5*$^{+}$ CP fields (Fig. 3A-D, insets). The notochord tip, labeled by *ntl*, was used as a morphological landmark for locating the adjacent CPs. Fluorescent dual *in situ* hybridization showed that *tmem88a* and *nkx2.5* transcripts colocalize in 8- and 14-somite stage embryos, confirming CP-specific *tmem88a* expression (Fig. 3E,F). Additionally, WISH for *tmem88a* was performed in similarly staged *cloche* mutant embryos, which lack progenitors for the hematovascular lineages. Transcript localization was identical in the ALPM of *cloche* mutants and wild-type embryos, indicating that, in the vicinity of *nkx2.5*$^{+}$ cells, *tmem88a* is expressed in precardiac fields and not in the presumptive endothelium (supplementary material Fig. S1). By 23-somites, however, the *tmem88a* transcript pattern becomes restricted to vascular tissue, including the endocardium and head vessels (supplementary material Fig. S2). Endothelial-specific expression persists until 48 hpf, after which point *tmem88a* transcripts are undetectable by WISH (data not shown). The expression of *tmem88a* in emerging CPs is consistent with an early role in cardiogenesis.

Depletion of Tmem88a from zebrafish embryos disrupts cardiogenesis

Loss-of-function studies were performed to determine whether *tmem88a* regulates cardiogenesis. Two morpholinos (MOs), a translation-blocker (tbMO) and a splice-site blocker (ssMO), were designed to target the *tmem88a* transcript (supplementary material Fig. S3A). Antibodies for validating the tbMO are not available. However, the effectiveness of the ssMO was confirmed by semi-quantitative RT-PCR. The native *tmem88a* transcript appeared to be eliminated in embryos injected with 8 or 12 ng ssMO (to the limit that we can detect using this strategy), and an aberrant unspliced variant accumulated (supplementary material Fig. S3B). The aberrant transcript was sequenced and found to encode a truncated and presumably dysfunctional protein. Individual injection of tbMO or ssMO into single-cell embryos caused 100% penetrant, identical and highly reproducible cardiac defects (supplementary material Fig. S4A). Co-injection of the MOs, each at subthreshold levels that did not individually perturb cardiogenesis, fully recapitulated this

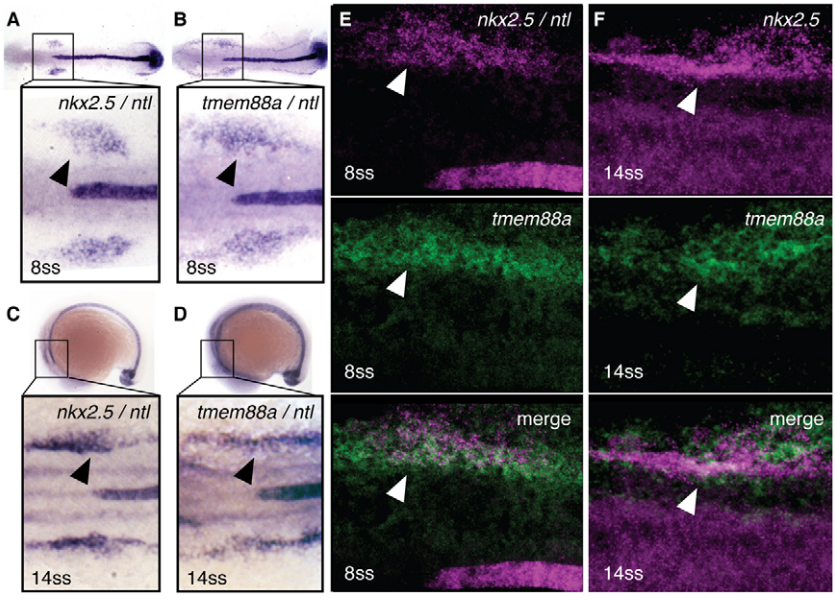

Fig. 3. *tmem88a* transcript localizes to cardiac progenitors. (**A**,**B**) Dorsal views (anterior to the left) of flatmount *in situ* hybridization of wild-type 8-somite stage zebrafish embryos stained for *nkx2.5/ntl* and *tmem88a/ntl*. Insets are higher magnifications of the boxed regions. (**C**,**D**) Laterals views of whole-mount *in situ* hybridization (WISH) preparations of wild-type 14-somite stage embryos stained for *nkx2.5/ntl* and *tmem88a/ntl*. Insets are higher magnification dorsal views of the boxed regions. (**E**,**F**) Dorsal views of cardiogenic mesoderm (anterior to the left) in flatmount dual fluorescent *in situ* hybridization preparations of wild-type embryos stained for *nkx2.5/ntl* or *tmem88a* at the 8- or 14-somite stage. Arrowheads indicate CPs. *n*>20 embryos analyzed per panel.

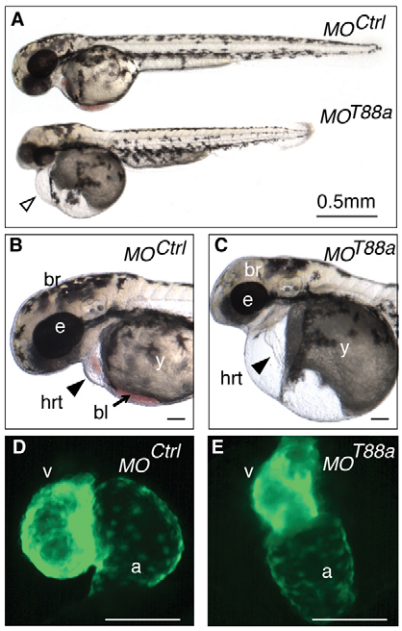

Fig. 4. Loss of Tmem88a results in profound cardiomyopathy. (**A**) Brightfield images of representative control (MO^{Ctrl}) and *tmem88a* (MO^{T88a}) morphants at 48 hpf. Arrowhead indicates pericardial edema. (**B**,**C**) Higher magnification of craniocardiac tissues in control and *tmem88a* morphants. Brain (br), eye (e), yolk (y), heart (hrt, arrowheads) and blood (bl, arrow) are indicated. (**D**,**E**) Fluorescent images of control and *tmem88a* morphant hearts observed in the *tg(myl7:eGFP)* background. Ventricle (v) and atrium (a) are indicated. *n*>50 embryos analyzed per panel. Scale bars: 0.1 mm in B-E.

phenotype, confirming the specificity of the *tmem88a* knockdown (supplementary material Fig. S4B). Morphologically, the *tmem88a*-related cardiac phenotype was first evident in 2-day-old embryos. At 28 hpf, control and *tmem88a* morphants were indistinguishable (supplementary material Fig. S5). However, by 48 hpf the *tmem88a* morphants had shortened trunks, reduced cranial features and pericardial edema (Fig. 4A). Closer examination revealed a lack of blood, a translucent heart-string and slowed heart rate (Fig. 4B,C; supplementary material Fig. S6).

Morphants were generated in the *tg(myl7:eGFP)* background, which expresses cardiomyocyte-specific eGFP. At 72 hpf, control hearts were fully looped, with adjacently positioned cardiac chambers of comparable size (Fig. 4D). By contrast, Tmem88a-deficient hearts were linear, and the cardiac chambers were reduced in size (Fig. 4E). These defects persisted until 7 days post-fertilization, at which point the embryos died. Similar cardiac defects, along with the absence of blood, were observed in $tp53^{M214K}$ mutants injected with *tmem88a* MOs (supplementary material Fig. S7), indicating that Tmem88a is required specifically for proper cardiogenesis and blood formation. We note that the cranial and truncal abnormalities were less pronounced in these embryos, so that partial off-target effects cannot be ruled out for those phenotypes.

Loss of Tmem88a causes hypocellularization of the heart

Cardiogenesis is an elaborate process that requires CP specification, cardiomyocyte differentiation, proliferation and morphogenesis. Cardiomyopathies can arise from failure at any of these stages. To better understand the requirement of Tmem88a for heart development, we analyzed heart cellularity in control and *tmem88a* morphants, derived from the *tg(myl7:DsRed2-nuc)* line, which expresses nuclear cardiomyocyte-specific DsRed2. At 51 hpf, embryonic hearts were dissected, immunostained and imaged to quantify cardiomyocyte cell numbers (Fig. 5A,B). Atrial, ventricular and total cardiomyocytes were counted (Fig. 5C). Depletion of Tmem88a causes a 30% reduction in total cardiomyocyte number. Atrial cardiomyocytes decrease by 20% and ventricular cells by 40%. The vertical length of the cardiac chambers was also measured (Fig. 5D). Morphant hearts were, on average, 30% shorter than those of controls.

Tmem88a regulates CP specification

The heart defects observed in *tmem88a* morphants could result from aberrations in CP specification, proliferation or cardiomyocyte differentiation. To assess cardiomyocyte differentiation, WISH was performed for differentiation markers in *tmem88a* and control morphants. *atrial myosin heavy chain* (*amhc*; *myh6* – Zebrafish Information Network) and *ventricular myosin heavy chain* (*vmhc*) were used to monitor atrial and ventricular development, respectively. At the 23-somite stage, control embryos showed the wild-type expression patterns of both markers (Fig. 6A,B). By contrast, *tmem88a* morphants had disrupted *amhc* and *vmhc* transcript patterns (Fig. 6C,D). The area of *vmhc* staining was reduced by 35%, and *amhc* staining was decreased by 45%

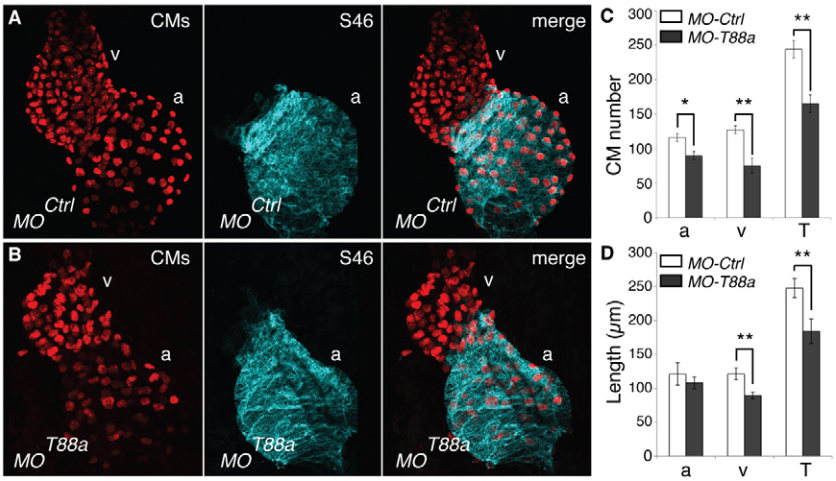

Fig. 5. Tmem88a-deficient hearts are small and hypocellular. (**A**,**B**) Representative confocal images of control and *tmem88a* morphant hearts dissected from 51 hpf zebrafish embryos. Morphants were generated in the *tg(myl7:DsRed2-nuc)* background. Left panels show immunohistochemistry for DsRed2 labeling of cardiomyocyte nuclei (CMs). Middle panels show S46 antibody labeling of atrial cells. Right panels show merge. Atrium (a) and ventricle (v) are indicated. (**C**) Atrial (a), ventricular (v) and total (T) cardiomyocyte numbers. (**D**) Atrial, ventricular and total cardiac chamber length. *n*=6 hearts quantified per condition. **P*<0.05, ***P*<0.01; error bars indicate s.d.

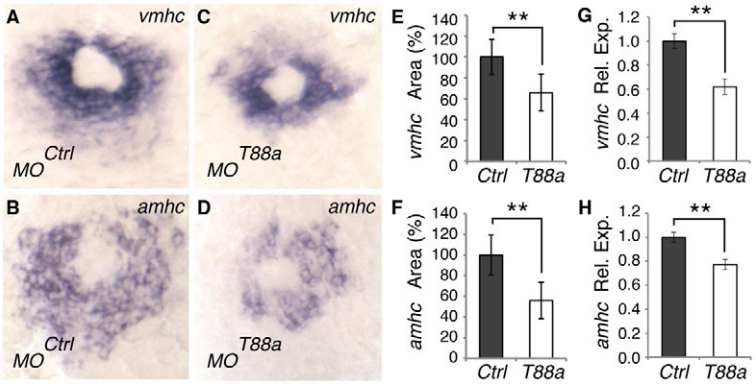

Fig. 6. *Tmem88a* depletion reduces the expression of cardiomyocyte differentiation markers. Zebrafish embryos were analyzed at the 23-somite stage. (**A-D**) WISH for ventricular cardiomyocyte marker (*vmhc*) and atrial cardiomyocyte marker (*amhc*) in control (A,B) and *tmem88a* (C,D) morphants. *n*>20 embryos analyzed per condition. (**E**,**F**) Relative *vmhc*$^+$ and *amhc*$^+$ areas in control (*Ctrl*) and *tmem88a* (*T88a*) morphants. (**G**,**H**) Relative expression levels of *vmhc* and *amhc* assessed by qPCR. Measurements are normalized to control; *n*=10 embryos measured per condition. ***P*<0.01; error bars indicate s.d.

(Fig. 6E,F). Relative expression analysis, as measured by qPCR, confirmed the reduction of both markers in Tmem88a-depleted embryos (Fig. 6G,H).

To determine whether the changes in differentiation marker expression were a consequence of defective CP specification, WISH was performed for the CP marker *nkx2.5*. As before, the rostral tip of the notochord was used as a landmark for orienting the normal *nkx2.5* expression domains. At the 8-somite stage, control morphants displayed the expected bilateral *nkx2.5* expression pattern (Fig. 7A). By contrast, identically staged *tmem88a* morphants had a significant reduction in the *nkx2.5*$^+$ domains (Fig. 7B). Using area measurements, we established that the *nkx2.5*$^+$ CP field was 60% smaller in *tmem88a* morphants than in controls (Fig. 7C). Relative expression analysis of *nkx2.5* by qPCR confirmed this reduction (Fig. 7D).

Since impaired CP specification might result from a more general mesodermal defect or loss of ALPM, we assessed the integrity of the ALPM in *tmem88a* morphants. Genes expressed throughout the ALPM include *gata4*, *gata5* and *tbx20* (Schoenebeck et al., 2007; Waxman et al., 2008). WISH revealed that the *gata4* expression pattern was identical in control and *tmem88a* morphants (Fig. 7E,F). In particular, the posterior boundary of the *gata4*$^+$ domains was located in the same position, as determined by measuring the distance from this boundary to the notochord tip, regardless of MO injection (Fig. 7G). Moreover, the relative expression level of *gata4* was unchanged in *tmem88a* morphants compared with controls (Fig. 7H). Given that the ALPM is unperturbed in Tmem88a-depleted embryos, the loss of *nkx2.5* expression implies that these embryos have a primary defect in CP specification.

Reduced CP specification in *tmem88a* morphants is not caused by increased apoptosis, decreased cell proliferation or fate conversion to the hematovascular or forelimb lineages

To establish whether the impaired CP specification in *tmem88a* morphants is due to defective cell cycle dynamics, apoptosis and cell proliferation assays were performed. Increased apoptosis was observed in the developing brain of *tmem88a* morphants compared with control embryos (data not shown). By contrast, no difference in apoptosis or cell proliferation was detected in the cardiogenic ALPM of control and *tmem88a* morphants (Fig. 8A-F).

The possibility of cell fate conversion was also considered. The heart develops in association with the hematovascular and forelimb organ fields (Schoenebeck et al., 2007; Van Handel et al., 2012; Waxman et al., 2008). During normal development, these non-cardiac domains limit the range of CP expansion. Moreover,

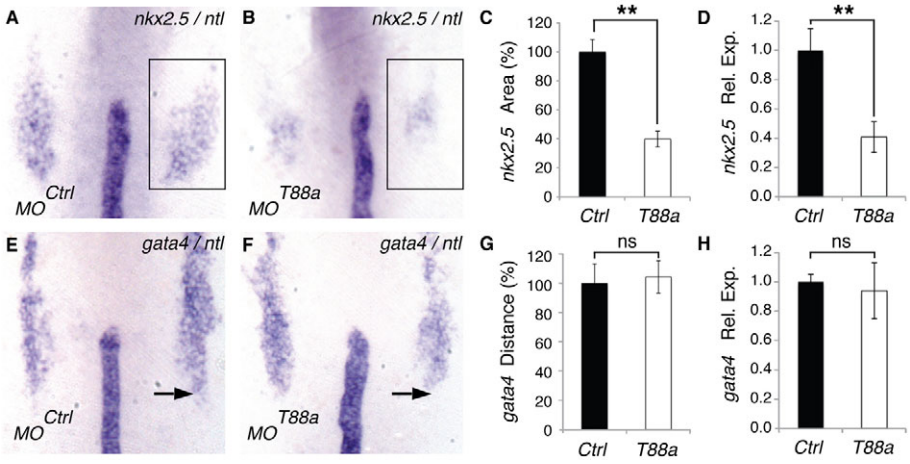

Fig. 7. Loss of Tmem88a reduces the CP fields. Zebrafish embryos were analyzed at the 8-somite stage. (**A**,**B**) WISH for *nkx2.5* (box) and *ntl* in representative control and *tmem88a* morphants. (**C**) Relative *nkx2.5*$^+$ areas in control and *tmem88a* morphants. (**D**) *nkx2.5* relative expression levels as assessed by qPCR. (**E**,**F**) WISH for *gata4* and *ntl* in representative control and *tmem88a* morphants. Arrow indicates the posterior *gata4*$^+$ domain boundary. (**G**) Relative distance between the notochord tip and the posterior *gata4*$^+$ domain boundary. (**H**) *gata4* relative expression levels by qPCR. (A,B,E,F) Dorsal views of flatmount embryos, with anterior to the top; *n*>20 embryos analyzed per condition. (C,G) Measurements are normalized to control; *n*=10 embryos measured per condition. ***P*<0.01; ns, not significant; error bars indicate s.d.

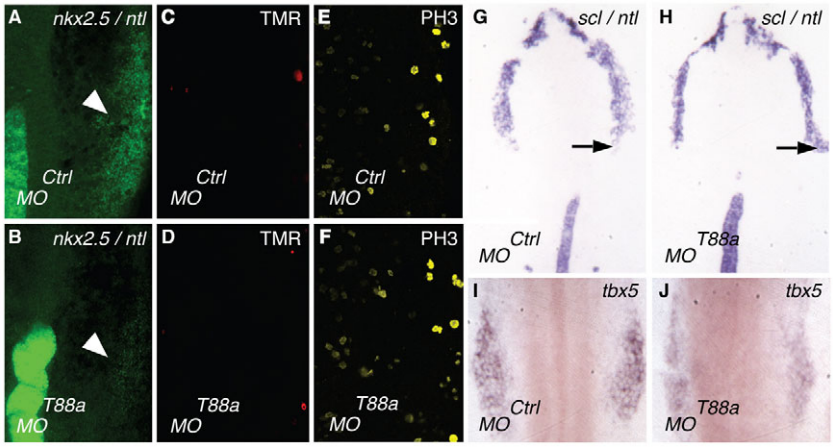

Fig. 8. Loss of CPs in *tmem88a* morphants is not caused by increased apoptosis, decreased cell proliferation or fate conversion to the hematovascular or forelimb lineages. Dorsal views of representative flatmount preparations of 8-somite (A-H) and 23-somite (I,J) control and *tmem88a* morphants, with anterior to the top (*n*>20 embryos analyzed per condition). (**A**,**B**) WISH for *nkx2.5* and *ntl*, showing the cardiogenic mesoderm (arrowheads). (**C**,**D**) Apoptosis detection by TMR-Red. (**E**,**F**) Phospho-Histone H3 antibody staining for cell proliferation. (**G**,**H**) WISH for the hematovascular marker *scl* and for *ntl*. Arrow indicates the boundary of the anterior *scl* expression domain. (**I**,**J**) WISH for the forelimb marker *tbx5*.

overexpression of the hematovascular transcription factor *scl* (*tal1* – Zebrafish Information Network) has been shown to convert precardiac mesoderm into blood and endothelium (Schoenebeck et al., 2007), indicating that fate conversion between neighboring organ fields is possible. To establish whether reduction in CP specification in *tmem88a* morphants is due to concomitant expansion of either hematovascular or forelimb tissues, we performed WISH for *scl* and *tbx5*. Neither the blood nor forelimb field was expanded in *tmem88a* morphants (Fig. 8G-J), indicating that the Tmem88a-related CP deficiency does not result from fate conversion to these lineages.

The requirement for appropriate Tmem88a levels is limited to cardiac and erythromyeloid precursors

Since the expression pattern of *tmem88a* in 8-somite stage embryos extends in the lateral mesoderm beyond the CP fields, we examined whether this gene is implicated in the development of other mesodermal tissues. WISH for the axial mesoderm marker *ntl*, paraxial mesoderm marker *myod* (*myod1* – Zebrafish Information Network), intermediate mesoderm marker *pax2a* and hematovascular marker *scl* indicated that the expression pattern of these genes was indistinguishable in *tmem88a* and control morphants (supplementary material Fig. S8A-H). However, the erythroid marker *gata1* was essentially undetectable in 75% of *tmem88a* morphants (supplementary material Fig. S8I,J). Analysis of additional hematopoietic and vascular markers showed that transcripts for *gata1* and the myeloid regulatory gene *pu1* (*spi1b* – Zebrafish Information Network) are reduced in *tmem88a* morphants compared with control embryos (supplementary material Fig. S8K). These findings are consistent with a recent publication documenting the requirement of Tmem88a in erythromyeloid development (Cannon et al., 2013). The selective loss of *gata1* and *pu1* expression in 8-somite stage morphants indicates an early role for Tmem88a in erythromyeloid precursor specification and/or blood lineage commitment downstream of the stem/progenitor regulatory gene *scl*.

WNT signaling negatively correlates with Tmem88a levels

Hematopoietic and cardiac development are regulated by WNT signaling. In both cases, a precisely timed sequence of WNT activation and inhibition is required for lineage commitment (Naito et al., 2006; Ueno et al., 2007). For instance, CP specification depends on WNT activity at or around gastrulation followed by WNT inhibition at the onset of somitogenesis. Interestingly, human TMEM88 was shown to negate a WNT overexpression phenotype when expressed in *Xenopus* explants (Lee et al., 2010). To establish whether zebrafish Tmem88a negatively regulates WNT activity during CP specification, we monitored the relative expression of a genetically engineered WNT sensor in response to Tmem88a expression. Using transgenic *TOPdGFP* reporter fish, WNT activity (GFP) was found to be elevated in *tmem88a* morphants and reduced in embryos injected with *tmem88a* mRNA, compared with controls (Fig. 9A,B). Similarly, the relative expression of the WNT target gene *dkk1* increased in *tmem88a* morphants and decreased in embryos injected with *tmem88a* mRNA, compared with controls (Fig. 9C,D). By contrast, control morphants and embryos injected with mutated *tmem88a* mRNA, which encodes a truncated protein lacking the C-terminal Val-Trp-Val motif, were unchanged for WNT-related gene expression. Therefore, active WNT signaling negatively correlates with Tmem88a levels during early somitogenesis.

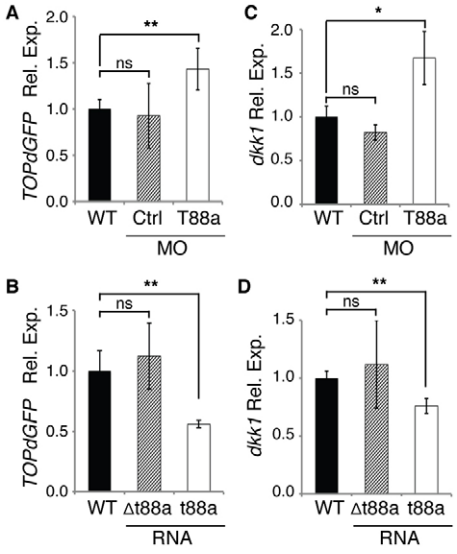

Fig. 9. WNT target gene expression negatively correlates with *tmem88a* levels. Relative expression levels assessed by qPCR of (**A**,**B**) the WNT sensor *TOPdGFP* and (**C**,**D**) the WNT target gene *dkk1* in wild-type zebrafish embryos (WT), in embryos injected with control (Ctrl) or *tmem88a* (T88a) MO, and in embryos injected with mutated *tmem88a* mRNA (Δt88a) or wild-type *tmem88a* mRNA (t88a). **P*<0.05, ***P*<0.01; ns, not significant; error bars indicate s.d.

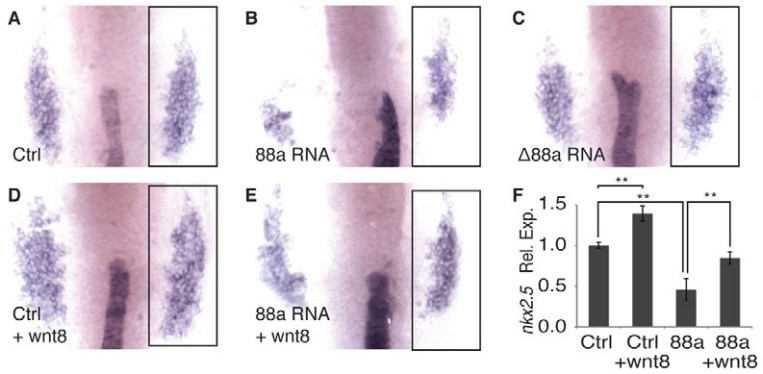

Fig. 10. CP formation is repressed by forced expression of wild-type but not mutant *tmem88a*, and this phenotype is rescued by enhancing early WNT signaling. (**A-E**) WISH for *nkx2.5* (box) and *ntl* in representative 8-somite stage uninjected control zebrafish embryos (A, Ctrl), embryos injected with wild-type *tmem88a* mRNA (B, 88a RNA), embryos injected with mutated *tmem88a* mRNA (C, Δ88a), heat-shocked uninjected control embryos (D, Ctrl+wnt8), and heat-shocked embryos that had been injected with wild-type *tmem88a* mRNA (E, 88a RNA+wnt8). Heat-shock treatment was administered to embryos at 3 hpf for 30 minutes. *n*>15 embryos analyzed per condition. (**F**) *nkx2.5* relative expression levels assessed by qPCR. ***P*<0.01; error bars indicate s.d.

Overexpression of *tmem88a* disrupts CP formation in a WNT-dependent manner

To evaluate whether the correlation between Tmem88a levels and WNT activity is significant to cardiogenesis, functional interactions were tested in the context of CP specification. Since CP specification requires the sequential activation and inhibition of WNT signaling, inappropriate modulation of the pathway should interfere with CP formation. For example, forced inhibition of WNT signaling by *dkk1* overexpression prior to 3.5 hpf reduces *nkx2.5* expression in 8-somite stage embryos (Ueno et al., 2007). Similarly, forced expression of Tmem88a by microinjection of mRNA caused a significant reduction in the *nkx2.5* expression pattern compared with wild-type controls (Fig. 10A,B) or control embryos injected with mutated *tmem88a* mRNA (Fig. 10C). By 48 hpf, embryos injected with wild-type *tmem88a* mRNA developed a discernable cardiomyopathy, whereas control embryos had morphologically normal hearts (supplementary material Fig. S9).

We reasoned that if the CP deficiency associated with *tmem88a* overexpression results from reduced levels of WNT signaling, forced WNT induction should rescue this phenotype. Rescue was attempted by injecting *tmem88a* mRNA into *tg(hsp70l:wnt8-eGFP)* embryos, which carry a heat-shock-inducible *wnt8* gene. Control and injected embryos were heat shocked at 3 hpf for 30 minutes and analyzed for *nkx2.5* expression at the 8-somite stage of development. Early induction of *wnt8* in wild-type embryos resulted in increased *nkx2.5* expression (Fig. 10D), as documented previously (Ueno et al., 2007). Interestingly, in embryos overexpressing *tmem88a*, forced WNT activation largely rescued the Tmem88a-induced CP deficiency (Fig. 10E,F). Since the deleterious effect of *tmem88a* overexpression on CP specification was reversed by increasing WNT signaling, Tmem88a and the WNT pathway appear to be antagonistic.

WNT signaling acts co-operatively with loss of Tmem88a to suppress CP specification

The *tmem88a* mRNA overexpression studies established antagonism between Tmem88a and WNT signaling, but did not determine the normal physiological relevance of this interaction. Expression of *tmem88a* is virtually undetectable until the end of gastrulation, a stage that coincides with procardiogenic inhibition of WNT activity. To establish whether *tmem88a* contributes to this inhibitory regulation, a combined MO and genetic approach was adopted. We reasoned that if Tmem88a is required for CP specification because it represses WNT activity, then increasing WNT signaling should sensitize embryos to the depletion of Tmem88a. To test this hypothesis, embryos derived from the *tg(hsp70l:wnt8-eGFP)* line were heat shocked for 30-60 minutes at 75% epiboly. This developmental stage was chosen because it follows mesoderm establishment but precedes the emergence of *nkx2.5*$^{+}$ CPs. A 60 minute heat-shock treatment caused significant depletion of *nkx2.5* in 8-somite stage control

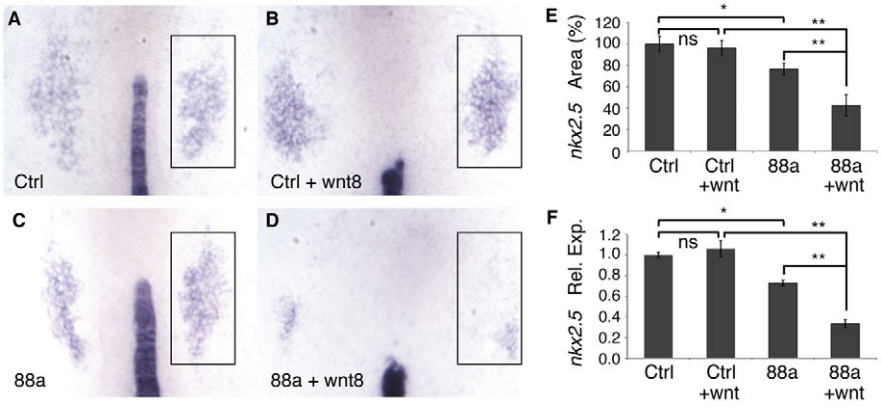

Fig. 11. Limited WNT signaling sensitizes cardiogenic mesoderm to subthreshold depletion of Tmem88a. (**A-D**) WISH for *nkx2.5* (box) and *ntl* in representative 8-somite stage control morphants (Ctrl) and subthreshold *tmem88a* morphants (88a), without or with (+wnt8) low-level WNT activation. Retraction of the notochord and general widening of the mesodermal plate occur in heat-shocked embryos, but independently of MO injection. Heat-shock treatment was administered to 75% epiboly embryos for 30 minutes. *n*>20 embryos analyzed per panel. (**E**) *nkx2.5*$^{+}$ area normalized to control values. *n*=10 embryos measured per condition. (**F**) *nkx2.5* relative expression levels assessed by qPCR. **P*<0.05, ***P*<0.01; ns, not significant; error bars indicate s.d.

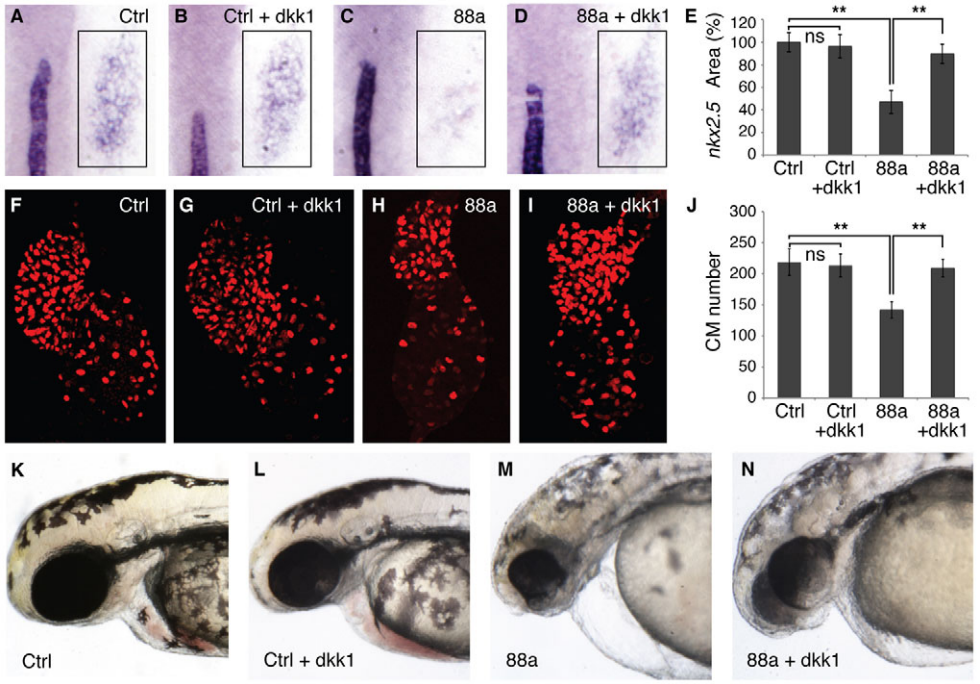

Fig. 12. Late suppression of WNT signaling rescues CPs and cardiomyocyte numbers in *tmem88a* morphants. (**A-D**) WISH for *nkx2.5* (box) and *ntl* in representative 8-somite stage control (Ctrl) and *tmem88a* (88a) morphants, without or with (+dkk1) WNT inhibition. Retraction of the notochord occurs in heat-shocked embryos, but independently of MO injection. Heat-shock treatment was administered to 75% epiboly embryos for 1 hour. *n*>20 embryos analyzed per panel. (**E**) *nkx2.5*$^{+}$ area normalized to control values. *n*=6 embryos measured per condition. (**F-I**) Cardiomyocyte nuclei in representative 48-hpf embryos from the *tg(myl7:DsRed2-nuc)* line. *n*>25 embryos analyzed per panel. (**J**) Quantification of total cardiomyocyte (CM) numbers. *n*=6 control hearts analyzed; *n*=9 hearts analyzed for all other conditions. (**K-N**) Brightfield images showing craniocardiac tissues in 48-hpf embryos. *n*>50 embryos analyzed per condition. ***P*<0.01; ns, not significant; error bars indicate s.d.

morphants, as previously reported (Ueno et al., 2007). By contrast, embryos treated for 30 minutes appeared identical to non-heat-shocked controls (Fig. 11A,B). Partial depletion of Tmem88a was accomplished using subthreshold quantities of *tmem88a* MO (1 ng). These embryos had only a moderate (25%) reduction in *nkx2.5* staining (Fig. 11C). A 30 minute heat-shock treatment of the partial morphants caused a profound (60-70%) deficiency in the *nkx2.5* expression domains, which was much more than the additive effect of the individual manipulations (Fig. 11D). These findings were quantified by measuring the area of *nkx2.5* expression under each condition, and using qPCR to determine *nkx2.5* relative expression levels (Fig. 11E,F). The synergistic repression of CP formation by *wnt8* overexpression and *tmem88a* depletion is consistent with a functional interaction between WNT signaling and Tmem88a activity.

Suppression of WNT signaling rescues the CP deficiency in *tmem88a* morphants

If loss of Tmem88a leads to enhanced WNT activity that blocks CP specification, then inhibition of WNT signaling just prior to specification should restore CP generation in the absence of Tmem88a. To test this idea, WNT signaling was downregulated using the *tg(hsp70l:dkk1-eGFP)* line to express the WNT inhibitor *dkk1* in a temporally specific manner. Control or *tmem88a* morphant embryos were heat shocked for 1 hour at 75% epiboly and CP formation was monitored by WISH for *nkx2.5*. In control embryos, WNT inhibition at this stage had no effect on the generation of nascent CPs (Fig. 12A,B). By contrast, the CP domains were rescued in 80% of the heat-shocked *tmem88a* morphants (Fig. 12C,D). These embryos had, on average, a 42% expansion of the *nkx2.5*$^{+}$ territories compared with non-heat-shocked *tmem88a* morphants, as quantified by area measurements and *nkx2.5* relative expression levels (Fig. 12E; supplementary material Fig. S10).

In addition to rescuing CP specification, *dkk1* overexpression resulted in complete recovery of total cardiomyocyte number in *tmem88a* morphants. Heat-shocked and non-heat-shocked control embryos had equivalent numbers of cardiomyocytes at 48 hpf (Fig. 12F,G). The 46% cardiomyocyte deficiency measured in *tmem88a* morphants was rescued upon *dkk1* overexpression (Fig. 12H-J). Cardiac morphology remained abnormal in these embryos, suggesting a separate or fine-tuned role for Tmem88a in morphogenesis. However, the rescue by *dkk1* expression was sufficient to cause a marked overall improvement in the gross craniocardiac morphology of the *tmem88a* morphants (Fig. 12K-N).

The WNT-dependent reversal of CP and cardiomyocyte loss in *tmem88a* morphants further supports a model whereby Tmem88a negatively modulates WNT signaling to create a permissive environment for cardiac progenitor specification, following an earlier WNT-dependent phase of cardiac mesoderm commitment.

DISCUSSION

Transcription factors and signaling pathways are important components of the cardiogenic network that drives CP specification, but the molecular details of the cross-regulation and balance among cues to ensure normal numbers of CPs remain largely unknown. WNT activation has previously been associated with reduced GATA factor expression (Afouda et al., 2008; Martin et al., 2010). In this study, we implicate GATA factors in limiting WNT signaling. We

identify *tmem88a* as a GATA-dependent gene that is required for the specification of normal numbers of cardiomyocytes. Either excessive or reduced *tmem88a* expression results in the disruption of *nkx2.5*$^{+}$ CP field size. Timed activation or inhibition of the WNT pathway rescues the *tmem88a* overexpression or loss-of-function phenotype, respectively. These observations provide strong evidence for a functional interaction between Tmem88a and the WNT pathway that is responsible, at least in part, for appropriate CP specification.

Given the major effect of *tmem88a* knockdown on CP specification, as measured by *nkx2.5* expression, it is somewhat surprising that later indicators of cardiac development, including differentiation markers and cardiomyocyte numbers, although altered significantly, were not more affected in *tmem88a* morphants. Since our morphant model is not null, one caveat is the transient nature of the *tmem88a* MO and potential recovery of Tmem88a levels. However, given the limited developmental window of action, this explanation seems unlikely. Another possibility is that neighboring cell populations compensate for the loss of *nkx2.5*$^{+}$ CPs in the developing morphants. Lineage-tracing studies have shown that *gata4*$^{+}$ *nkx2.5*$^{-}$ head mesenchyme progenitors, positioned anterior to the *nkx2.5*$^{+}$ CPs, can replace ablated CPs in 18-somite stage or younger embryos (Serbedzija et al., 1998). Since the *gata4*$^{+}$ ALPM is intact in *tmem88a* morphants, these head mesenchyme progenitors might compensate and partially rescue the post-specification stages of cardiogenesis. Since tissue-specific markers for these cells are not available, the size of the head mesenchyme progenitor field cannot be quantified using WISH, and lineage-tracing experiments will be needed to test this hypothesis. Another unanswered question relates to the fate, in *tmem88a* morphants, of the *gata4*$^{+}$ cells that are normally cardiogenic. We did not observe increased cell death or decreased cell proliferation in or near the *nkx2.5*$^{+}$ ALPM of *tmem88a* morphants. Nor was there any expansion in the hematovascular or forelimb fields that are normally adjacent to the precardiac mesoderm. Again, with the development of appropriate reporter lines, lineage-tracing experiments might help to identify the fate of the cells that fail to express *nkx2.5* in embryos lacking Tmem88a function.

Tmem88a is the second small transmembrane protein of unknown function (TMEM) to be implicated in cardiogenesis. Recent forward genetic screens identified Tmem2 as a protein involved in cardiomyocyte migration and atrioventricular canal formation (Smith et al., 2011; Totong et al., 2011). Tmem2 was shown to act by negatively modulating BMP signaling. Although Tmem2 and Tmem88a share no homology, they are both transmembrane proteins that inhibit important signaling pathways, most likely by sequestering key pathway components at the plasma membrane. Our findings suggest that Tmem88a is much less effective at WNT repression than Dkk1, a soluble WNT inhibitor. The effect of Tmem2 on BMP activation also seems moderate (Smith et al., 2011; Totong et al., 2011). TMEM proteins might therefore constitute a novel regulatory layer that is responsible for the fine-tuning of major signaling cascades in cardiogenesis.

Although we identified *tmem88a* as a regulator of CP specification, this gene is also involved in the development of erythromyeloid tissue. Cannon et al. recently showed that erythroid and myeloid cell numbers are significantly decreased in *tmem88a* morphants at 48 hpf, compared with wild-type embryos (Cannon et al., 2013). We observed that 8-somite stage *tmem88a* morphants had markedly reduced expression levels of the erythroid progenitor marker *gata1* and the myeloid progenitor marker *pu1*. Thus, Tmem88a is likely to be required for the specification or differentiation of a common erythromyeloid precursor cell. Interestingly, *dkk1* overexpression did not rescue the blood deficiency in *tmem88a* morphants, and so the mechanism of action of Tmem88a in hematopoietic development remains unclear.

Acknowledgements
We thank Timothy Hla for access to the LSM510 confocal microscope and the staff at the WCMC Optical Microscopy Core for imaging support; Wolfram Goessling for providing the *cloche* mutants and the *tg(hsp70l:wnt8-eGFP)*, *tg(hsp70l:dkk-eGFP)* and *TOPdGFP* transgenic lines; Yariv Houvras for providing the *tp53*^{M214K} mutant line; Fabien Campagne and Christopher Mason for advice during the next generation sequencing screen; members of the Caroline Burns and Wolfram Goessling laboratories for invaluable technical advice; Yariv Houvras and members of the T.E. laboratory for thoughtful critiques of the work; and the Weill Cornell/Rockefeller/Sloan-Kettering MD-PhD Program for support and mentorship.

Funding
This work was supported by the National Institutes of Health [HL111400 to T.E.; and Medical Scientist Training Program grant GM07739 to N.N.]. Deposited in PMC for release after 12 months.

Competing interests statement
The authors declare no competing financial interests.

Author contributions
N.N. designed the study, carried out all the experiments and wrote the manuscript. T.E. designed the study and wrote the manuscript.

Supplementary material
Supplementary material available online at
http://dev.biologists.org/lookup/suppl/doi:10.1242/dev.093567/-/DC1

References

Afouda, B. A., Martin, J., Liu, F., Ciau-Uitz, A., Patient, R. and Hoppler, S. (2008). GATA transcription factors integrate Wnt signalling during heart development. *Development* **135**, 3185-3190.
Anders, S. and Huber, W. (2010). Differential expression analysis for sequence count data. *Genome Biol.* **11**, R106.
Berghmans, S., Murphey, R. D., Wienholds, E., Neuberg, D., Kutok, J. L., Fletcher, C. D., Morris, J. P., Liu, T. X., Schulte-Merker, S., Kanki, J. P. et al. (2005). tp53 mutant zebrafish develop malignant peripheral nerve sheath tumors. *Proc. Natl. Acad. Sci. USA* **102**, 407-412.
Black, B. L. (2007). Transcriptional pathways in second heart field development. *Semin. Cell Dev. Biol.* **18**, 67-76.
Brand, T. (2003). Heart development: molecular insights into cardiac specification and early morphogenesis. *Dev. Biol.* **258**, 1-19.
Brend, T. and Holley, S. A. (2009). Zebrafish whole mount high-resolution double fluorescent in situ hybridization. *J. Vis. Exp.* **25**, pii:1229.
Buckingham, M., Meilhac, S. and Zaffran, S. (2005). Building the mammalian heart from two sources of myocardial cells. *Nat. Rev. Genet.* **6**, 826-837.
Cai, C. L., Liang, X., Shi, Y., Chu, P. H., Pfaff, S. L., Chen, J. and Evans, S. (2003). Isl1 identifies a cardiac progenitor population that proliferates prior to differentiation and contributes a majority of cells to the heart. *Dev. Cell* **5**, 877-889.
Cannon, J. E., Place, E. S., Eve, A. M. J., Bradshaw, C. R., Sesay, A., Morrell, N. W. and Smith, J. C. (2013). Global analysis of the haematopoietic and endothelial transcriptome during zebrafish development. *Mech. Dev.* **130**, 122-131.
Chen, J. N. and Fishman, M. C. (1996). Zebrafish tinman homolog demarcates the heart field and initiates myocardial differentiation. *Development* **122**, 3809-3816.
Dorff, K. C., Chambwe, N., Zeno, Z., Shaknovich, R. and Campagne, F. (2012). GobyWeb: simplified management and analysis of gene expression and DNA methylation sequencing data. *Quantitative Methods* arXiv:1211.6666.
Dorsky, R. I., Sheldahl, L. C. and Moon, R. T. (2002). A transgenic Lef1/beta-catenin-dependent reporter is expressed in spatially restricted domains throughout zebrafish development. *Dev. Biol.* **241**, 229-237.
Evans, S. M., Yelon, D., Conlon, F. L. and Kirby, M. L. (2010). Myocardial lineage development. *Circ. Res.* **107**, 1428-1444.
Foley, A. C., Gupta, R. W., Guzzo, R. M., Korol, O. and Mercola, M. (2006). Embryonic heart induction. *Ann. N. Y. Acad. Sci.* **1080**, 85-96.

Hami, D., Grimes, A. C., Tsai, H. J. and Kirby, M. L. (2011). Zebrafish cardiac development requires a conserved secondary heart field. *Development* **138**, 2389-2398.
Harvey, R. P. (2002). Patterning the vertebrate heart. *Nat. Rev. Genet.* **3**, 544-556.
Heicklen-Klein, A. and Evans, T. (2004). T-box binding sites are required for activity of a cardiac GATA-4 enhancer. *Dev. Biol.* **267**, 490-504.
Holtzinger, A. and Evans, T. (2007). Gata5 and Gata6 are functionally redundant in zebrafish for specification of cardiomyocytes. *Dev. Biol.* **312**, 613-622.
Huang, C. J., Tu, C. T., Hsiao, C. D., Hsieh, F. J. and Tsai, H. J. (2003). Germ-line transmission of a myocardium-specific GFP transgene reveals critical regulatory elements in the cardiac myosin light chain 2 promoter of zebrafish. *Dev. Dyn.* **228**, 30-40.
Huang, W., Sherman, B. T. and Lempicki, R. A. (2009a). Bioinformatics enrichment tools: paths toward the comprehensive functional analysis of large gene lists. *Nucleic Acids Res.* **37**, 1-13.
Huang, W., Sherman, B. T. and Lempicki, R. A. (2009b). Systematic and integrative analysis of large gene lists using DAVID bioinformatics resources. *Nat. Protoc.* **4**, 44-57.
Ieda, M., Fu, J. D., Delgado-Olguin, P., Vedantham, V., Hayashi, Y., Bruneau, B. G. and Srivastava, D. (2010). Direct reprogramming of fibroblasts into functional cardiomyocytes by defined factors. *Cell* **142**, 375-386.
Jowett, T. (1998). Analysis of protein and gene expression. *Methods Cell Biol.* **59**, 63-85.
Keegan, B. R., Meyer, D. and Yelon, D. (2004). Organization of cardiac chamber progenitors in the zebrafish blastula. *Development* **131**, 3081-3091.
Kelly, R. G., Brown, N. A. and Buckingham, M. E. (2001). The arterial pole of the mouse heart forms from Fgf10-expressing cells in pharyngeal mesoderm. *Dev. Cell* **1**, 435-440.
Kimmel, C. B., Ballard, W. W., Kimmel, S. R., Ullmann, B. and Schilling, T. F. (1995). Stages of embryonic development of the zebrafish. *Dev. Dyn.* **203**, 253-310.
Klinedinst, S. L. and Bodmer, R. (2003). Gata factor Pannier is required to establish competence for heart progenitor formation. *Development* **130**, 3027-3038.
Krauss, S., Johansen, T., Korzh, V., Moens, U., Ericson, J. U. and Fjose, A. (1991). Zebrafish pax[zf-a]: a paired box-containing gene expressed in the neural tube. *EMBO J.* **10**, 3609-3619.
Kwon, C., Arnold, J., Hsiao, E. C., Taketo, M. M., Conklin, B. R. and Srivastava, D. (2007). Canonical Wnt signaling is a positive regulator of mammalian cardiac progenitors. *Proc. Natl. Acad. Sci. USA* **104**, 10894-10899.
Lavery, D. L., Martin, J., Turnbull, Y. D. and Hoppler, S. (2008). Wnt6 signaling regulates heart muscle development during organogenesis. *Dev. Biol.* **323**, 177-188.
Lee, H. J., Finkelstein, D., Li, X., Wu, D., Shi, D. L. and Zheng, J. J. (2010). Identification of transmembrane protein 88 (TMEM88) as a dishevelled-binding protein. *J. Biol. Chem.* **285**, 41549-41556.
Li, H. and Durbin, R. (2009). Fast and accurate short read alignment with Burrows-Wheeler transform. *Bioinformatics* **25**, 1754-1760.
Liao, E. C., Paw, B. H., Oates, A. C., Pratt, S. J., Postlethwait, J. H. and Zon, L. I. (1998). SCL/Tal-1 transcription factor acts downstream of cloche to specify hematopoietic and vascular progenitors in zebrafish. *Genes Dev.* **12**, 621-626.
Liu, W. and Foley, A. C. (2011). Signaling pathways in early cardiac development. *Wiley Interdiscip. Rev. Syst. Biol. Med.* **3**, 191-205.
Livak, K. J. and Schmittgen, T. D. (2001). Analysis of relative gene expression data using real-time quantitative PCR and the 2(-Delta Delta C(T)) method. *Methods* **25**, 402-408.
Lou, X., Deshwar, A. R., Crump, J. G. and Scott, I. C. (2011). Smarcd3b and Gata5 promote a cardiac progenitor fate in the zebrafish embryo. *Development* **138**, 3113-3123.
Lough, J. and Sugi, Y. (2000). Endoderm and heart development. *Dev. Dyn.* **217**, 327-342.
Mably, J. D., Mohideen, M. A., Burns, C. G., Chen, J. N. and Fishman, M. C. (2003). heart of glass regulates the concentric growth of the heart in zebrafish. *Curr. Biol.* **13**, 2138-2147.
Martin, J., Afouda, B. A. and Hoppler, S. (2010). Wnt/beta-catenin signalling regulates cardiomyogenesis via GATA transcription factors. *J. Anat.* **216**, 92-107.
Meilhac, S. M., Esner, M., Kelly, R. G., Nicolas, J. F. and Buckingham, M. E. (2004). The clonal origin of myocardial cells in different regions of the embryonic mouse heart. *Dev. Cell* **6**, 685-698.
Mjaatvedt, C. H., Nakaoka, T., Moreno-Rodriguez, R., Norris, R. A., Kern, M. J., Eisenberg, C. A., Turner, D. and Markwald, R. R. (2001). The outflow tract of the heart is recruited from a novel heart-forming field. *Dev. Biol.* **238**, 97-109.
Naito, A. T., Shiojima, I., Akazawa, H., Hidaka, K., Morisaki, T., Kikuchi, A. and Komuro, I. (2006). Developmental stage-specific biphasic roles of Wnt/beta-catenin signaling in cardiomyogenesis and hematopoiesis. *Proc. Natl. Acad. Sci. USA* **103**, 19812-19817.
Paige, S. L., Osugi, T., Afanasiev, O. K., Pabon, L., Reinecke, H. and Murry, C. E. (2010). Endogenous Wnt/beta-catenin signaling is required for cardiac differentiation in human embryonic stem cells. *PLoS ONE* **5**, e11134.
Patient, R. K. and McGhee, J. D. (2002). The GATA family (vertebrates and invertebrates). *Curr. Opin. Genet. Dev.* **12**, 416-422.
Ragkousi, K., Beh, J., Sweeney, S., Starobinska, E. and Davidson, B. (2011). A single GATA factor plays discrete, lineage specific roles in ascidian heart development. *Dev. Biol.* **352**, 154-163.
Reiter, J. F., Alexander, J., Rodaway, A., Yelon, D., Patient, R., Holder, N. and Stainier, D. Y. (1999). Gata5 is required for the development of the heart and endoderm in zebrafish. *Genes Dev.* **13**, 2983-2995.
Saga, Y., Kitajima, S. and Miyagawa-Tomita, S. (2000). Mesp1 expression is the earliest sign of cardiovascular development. *Trends Cardiovasc. Med.* **10**, 345-352.
Schoenebeck, J. J., Keegan, B. R. and Yelon, D. (2007). Vessel and blood specification override cardiac potential in anterior mesoderm. *Dev. Cell* **13**, 254-267.
Schulte-Merker, S., Ho, R. K., Herrmann, B. G. and Nüsslein-Volhard, C. (1992). The protein product of the zebrafish homologue of the mouse T gene is expressed in nuclei of the germ ring and the notochord of the early embryo. *Development* **116**, 1021-1032.
Serbedzija, G. N., Chen, J. N. and Fishman, M. C. (1998). Regulation in the heart field of zebrafish. *Development* **125**, 1095-1101.
Singh, M. K., Li, Y., Li, S., Cobb, R. M., Zhou, D., Lu, M. M., Epstein, J. A., Morrisey, E. E. and Gruber, P. J. (2010). Gata4 and Gata5 cooperatively regulate cardiac myocyte proliferation in mice. *J. Biol. Chem.* **285**, 1765-1772.
Smith, K. A., Lagendijk, A. K., Courtney, A. D., Chen, H., Paterson, S., Hogan, B. M., Wicking, C. and Bakkers, J. (2011). Transmembrane protein 2 (Tmem2) is required to regionally restrict atrioventricular canal boundary and endocardial cushion development. *Development* **138**, 4193-4198.
Sprague, J., Bayraktaroglu, L., Clements, D., Conlin, T., Fashena, D., Frazer, K., Haendel, M., Howe, D. G., Mani, P., Ramachandran, S. et al. (2006). The Zebrafish Information Network: the zebrafish model organism database. *Nucleic Acids Res.* **34**, D581-D585.
Sprague, J., Bayraktaroglu, L., Bradford, Y., Conlin, T., Dunn, N., Fashena, D., Frazer, K., Haendel, M., Howe, D. G., Knight, J. et al. (2008). The Zebrafish Information Network: the zebrafish model organism database provides expanded support for genotypes and phenotypes. *Nucleic Acids Res.* **36**, D768-D772.
Stainier, D. Y. (2001). Zebrafish genetics and vertebrate heart formation. *Nat. Rev. Genet.* **2**, 39-48.
Stainier, D. Y., Weinstein, B. M., Detrich, H. W., 3rd, Zon, L. I. and Fishman, M. C. (1995). Cloche, an early acting zebrafish gene, is required by both the endothelial and hematopoietic lineages. *Development* **121**, 3141-3150.
Stoick-Cooper, C. L., Weidinger, G., Riehle, K. J., Hubbert, C., Major, M. B., Fausto, N. and Moon, R. T. (2007). Distinct Wnt signaling pathways have opposing roles in appendage regeneration. *Development* **134**, 479-489.
Takeuchi, J. K. and Bruneau, B. G. (2009). Directed transdifferentiation of mouse mesoderm to heart tissue by defined factors. *Nature* **459**, 708-711.
Thomas, N. A., Koudijs, M., van Eeden, F. J., Joyner, A. L. and Yelon, D. (2008). Hedgehog signaling plays a cell-autonomous role in maximizing cardiac developmental potential. *Development* **135**, 3789-3799.
Totong, R., Schell, T., Lescroart, F., Ryckebüsch, L., Lin, Y. F., Zygmunt, T., Herwig, L., Krudewig, A., Gershoony, D., Belting, H. G. et al. (2011). The novel transmembrane protein Tmem2 is essential for coordination of myocardial and endocardial morphogenesis. *Development* **138**, 4199-4205.
Tzahor, E. (2007). Wnt/beta-catenin signaling and cardiogenesis: timing does matter. *Dev. Cell* **13**, 10-13.
Ueno, S., Weidinger, G., Osugi, T., Kohn, A. D., Golob, J. L., Pabon, L., Reinecke, H., Moon, R. T. and Murry, C. E. (2007). Biphasic role for Wnt/beta-catenin signaling in cardiac specification in zebrafish and embryonic stem cells. *Proc. Natl. Acad. Sci. USA* **104**, 9685-9690.
Van Handel, B., Montel-Hagen, A., Sasidharan, R., Nakano, H., Ferrari, R., Boogerd, C. J., Schredelseker, J., Wang, Y., Hunter, S., Org, T. et al. (2012). Scl represses cardiomyogenesis in prospective hemogenic endothelium and endocardium. *Cell* **150**, 590-605.
Vincent, S. D. and Buckingham, M. E. (2010). How to make a heart: the origin and regulation of cardiac progenitor cells. *Curr. Top. Dev. Biol.* **90**, 1-41.
Waldo, K. L., Kumiski, D. H., Wallis, K. T., Stadt, H. A., Hutson, M. R., Platt, D. H. and Kirby, M. L. (2001). Conotruncal myocardium arises from a secondary heart field. *Development* **128**, 3179-3188.
Waxman, J. S., Keegan, B. R., Roberts, R. W., Poss, K. D. and Yelon, D. (2008). Hoxb5b acts downstream of retinoic acid signaling in the forelimb field to restrict heart field potential in zebrafish. *Dev. Cell* **15**, 923-934.
Weidinger, G., Thorpe, C. J., Wuennenberg-Stapleton, K., Ngai, J. and Moon, R. T. (2005). The Sp1-related transcription factors sp5 and sp5-like act

downstream of Wnt/beta-catenin signaling in mesoderm and neuroectoderm patterning. *Curr. Biol.* **15**, 489-500.
Weinberg, E. S., Allende, M. L., Kelly, C. S., Abdelhamid, A., Murakami, T., Andermann, P., Doerre, O. G., Grunwald, D. J. and Riggleman, B. (1996). Developmental regulation of zebrafish MyoD in wild-type, no tail and spadetail embryos. *Development* **122**, 271-280.
Witzel, H. R., Jungblut, B., Choe, C. P., Crump, J. G., Braun, T. and Dobreva, G. (2012). The LIM protein Ajuba restricts the second heart field progenitor pool by regulating Isl1 activity. *Dev. Cell* **23**, 58-70.
Yang, J. and Xu, X. (2012). Immunostaining of dissected zebrafish embryonic heart. *J. Vis. Exp.* **59**, e3510.
Zaffran, S., Kelly, R. G., Meilhac, S. M., Buckingham, M. E. and Brown, N. A. (2004). Right ventricular myocardium derives from the anterior heart field. *Circ. Res.* **95**, 261-268.
Zhao, R., Watt, A. J., Battle, M. A., Li, J., Bondow, B. J. and Duncan, S. A. (2008). Loss of both GATA4 and GATA6 blocks cardiac myocyte differentiation and results in acardia in mice. *Dev. Biol.* **317**, 614-619.
Zhou, Y., Cashman, T. J., Nevis, K. R., Obregon, P., Carney, S. A., Liu, Y., Gu, A., Mosimann, C., Sondalle, S., Peterson, R. E. et al. (2011). Latent TGF-β binding protein 3 identifies a second heart field in zebrafish. *Nature* **474**, 645-648.
Zhou, P., He, A. and Pu, W. T. (2012). Regulation of GATA4 transcriptional activity in cardiovascular development and disease. *Curr. Top. Dev. Biol.* **100**, 143-169.

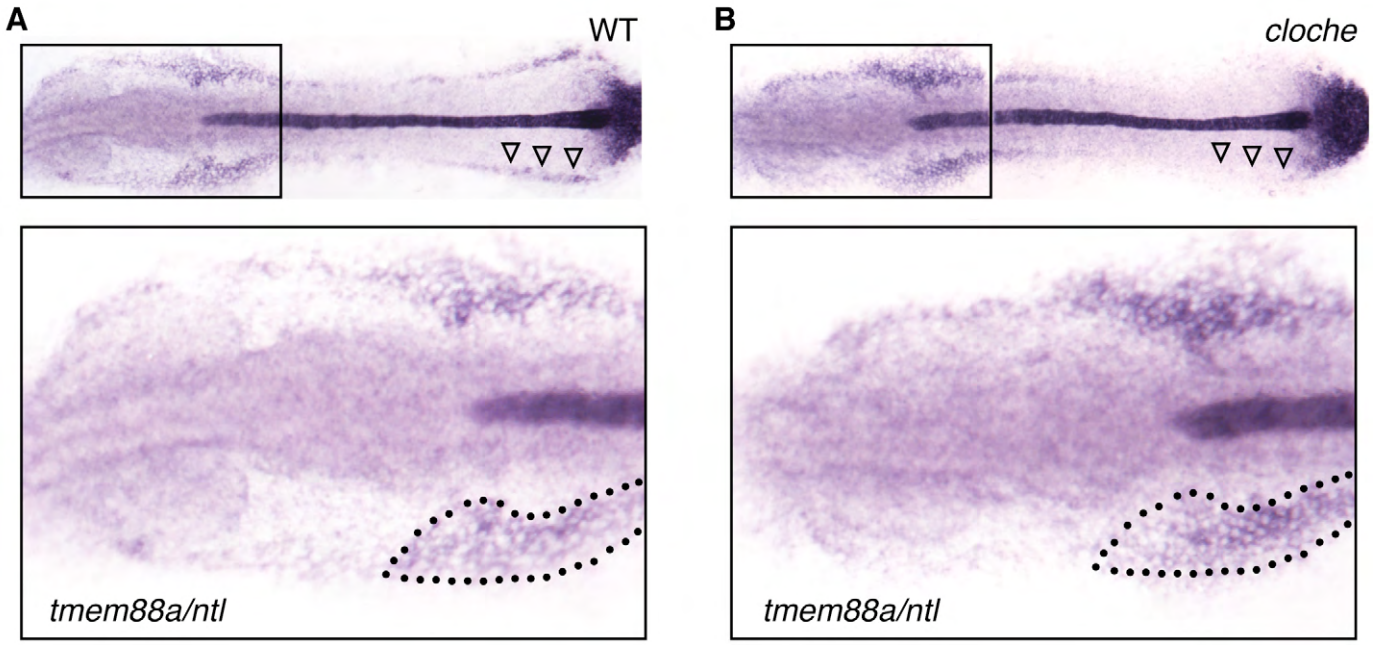

Fig. S1. Analysis of *tmem88a* expression in embryos lacking hematovascular progenitors. WISH for *tmem88a* and the notochord marker *ntl* in sibling (**A**) wild-type (WT) (*n*=17) and (**B**) *cloche* (*n*=6) embryos at the 10-somite stage. Shown are dorsal views of flat-mounted embryos, with anterior to the left. Homozygous *cloche* mutants lack *tmem88a* expression in the hematovascular region of the posterior lateral plate mesoderm (arrowheads). By contrast, as confirmed in higher magnification views of boxed areas, *tmem88a* transcript patterns are normal in the ALPM of *cloche* mutants compared with sibling wild-type embryos (insets, dotted lines).

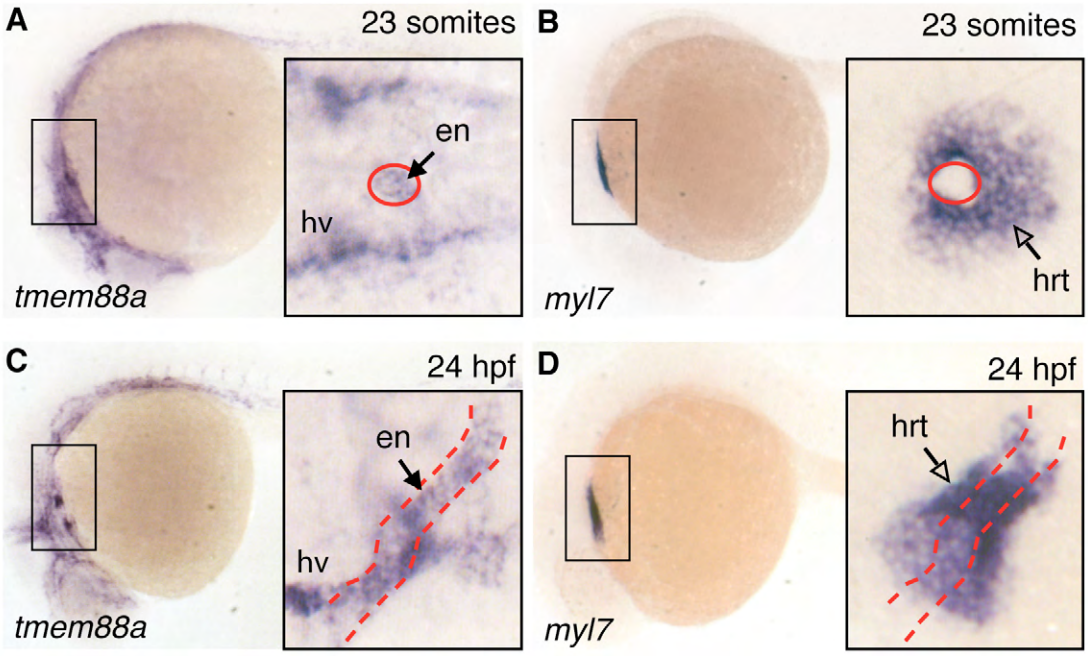

Fig S2. At later stages, *tmem88a* transcripts localize to endothelium. WISH in representative wild-type embryos for *tmem88a* and *myl7* transcript localization. (**A**,**B**) Representative 23-somite stage and (**C**,**D**) 24-hpf embryos are shown with anterior to the left. Lateral views in each panel are supplemented with higher magnification dorsal views of the boxed regions (insets). Endothelial tissues, including endocardium (en, red dashed outline) and head vessels (hv) express the *tmem88a* transcript, whereas *myl7* is restricted to the heart muscle (hrt, open arrow). All insets are shown at the same magnification. *n*>20 embryos analyzed per panel.

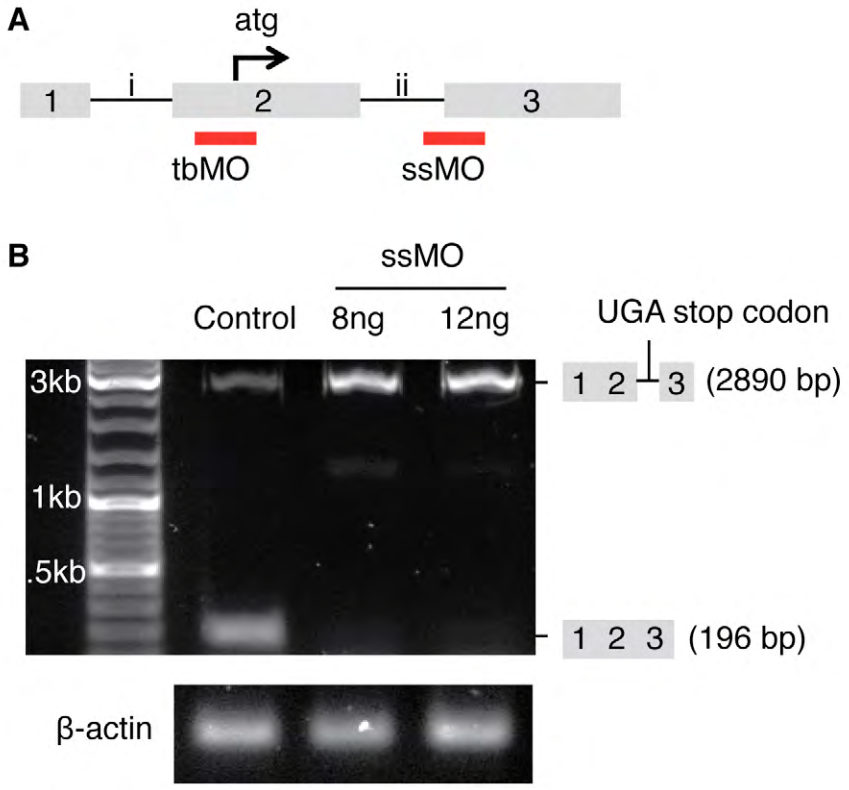

Fig. S3. Design and validation of *tmem88a* morpholinos. (**A**) Morpholino design. A translation blocker (tbMO) was targeted to the translation start site (atg) of *tmem88a* mRNA. A splice-site blocker (ssMO) was targeted to the boundary between intron 2 (ii) and exon 3 (3) of the mRNA. (**B**) The efficacy of the ssMO was monitored by semi-quantitative reverse-transcription PCR. The abundance of the normal *tmem88a* transcript (196 bp) was reduced with optimal doses of ssMO. An unspliced transcript (2890 bp) accumulated that is predicted to encode a premature stop codon (UGA), confirmed by sequencing. Levels of β-*actin* were used as a loading control.

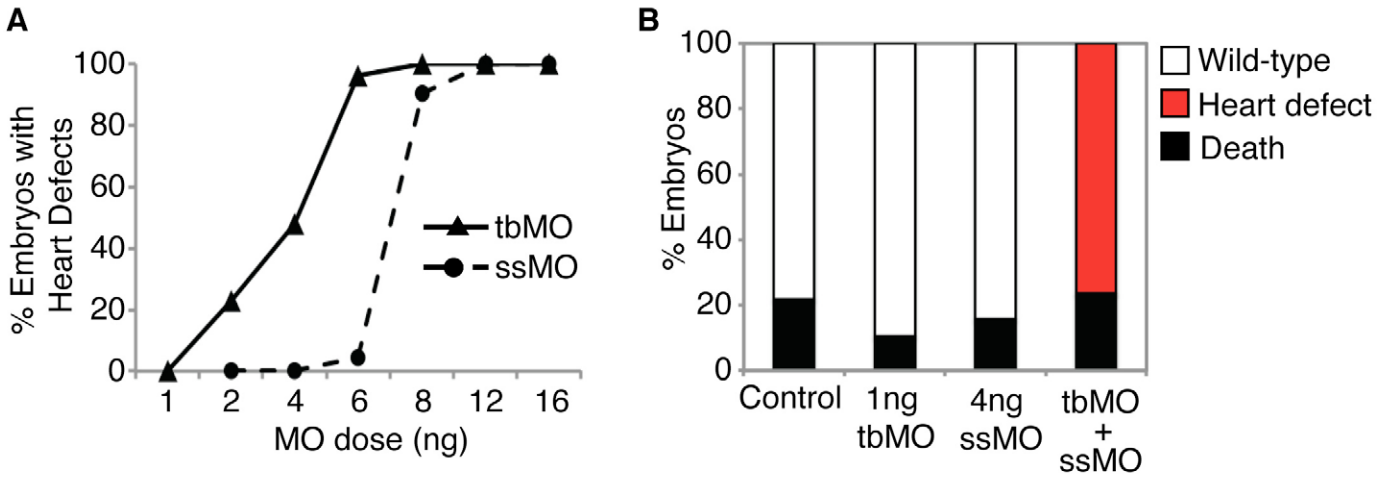

Fig. S4. Heart defects in *tmem88a* morphants are specific to Tmem88a knockdown. (**A**) Titrations of *tmem88a* translation-blocking morpholino (tbMO) and splice site-blocking morpholino (ssMO) establish the optimal morpholino dose (6 or 8 ng, respectively) for generating consistent heart defects. Note that this amount of ssMO is sufficient to essentially eliminate the normal transcript (see Fig. S3). (**B**) Suboptimal amounts of the two MOs (1 ng tbMO and 4 ng ssMO) on their own did not cause cardiac phenotypes. However, when combined, these were sufficient together to effectively phenocopy individual above-threshold morphants, confirming that morphant heart defects are specific to loss of Tmem88a.

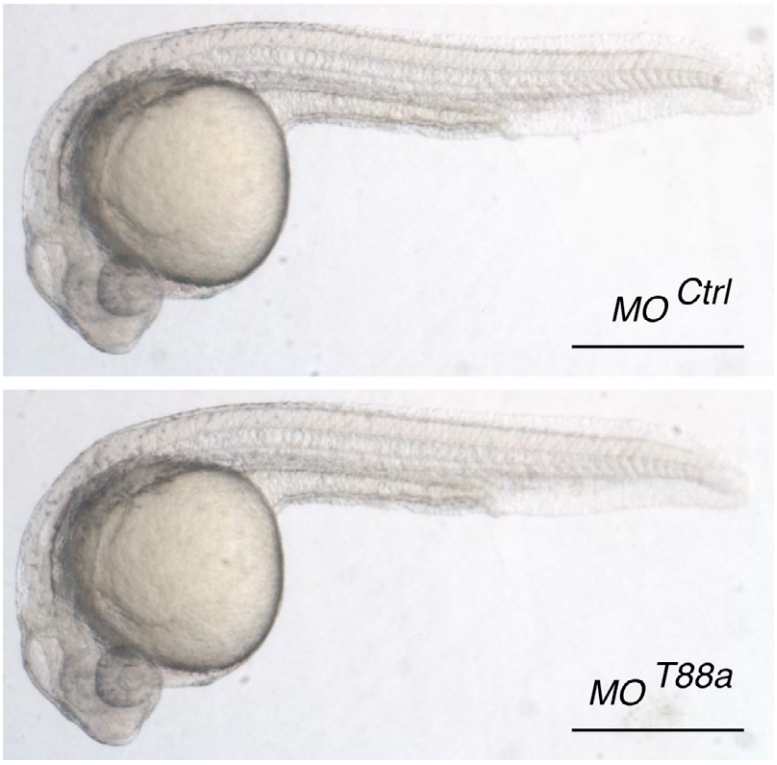

Fig. S5. Control and *tmem88a* morphants are morphologically similar at 28 hpf. Representative control (MO^{Ctrl}) and *tmem88a* (MO^{T88a}) morphants shown at 28 hpf; lateral views, anterior to the left. n>50 embryos analyzed per panel. Scale bar: 0.5 mm.

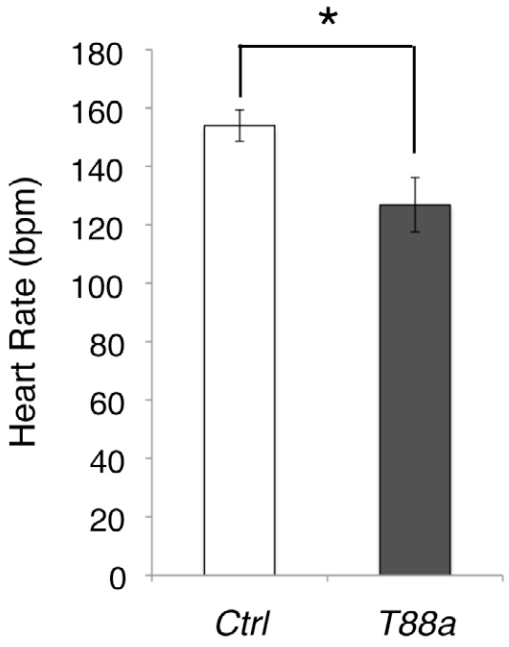

Fig. S6. Heart rate is reduced in *tmem88a* morphants. Heart rate in 48-hpf control (*Ctrl*) and *tmem88a* morphants (*T88a*) measured in beats per minute (bpm). n=20 embryos quantified per condition. *P<0.05.

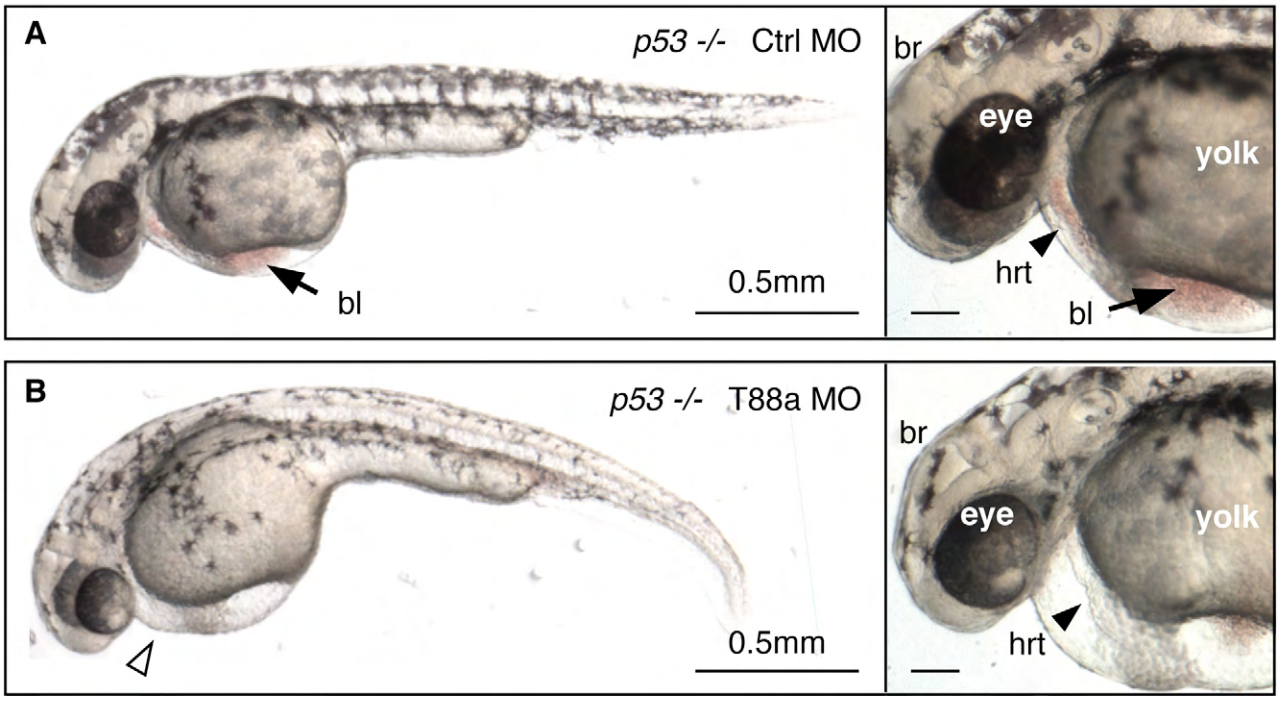

Fig. S7. The cardiomyopathy caused by depletion of Tmem88a is p53 independent. Brightfield images of representative 48-hpf *p53*$^{-/-}$ embryos injected with (**A**) control (Ctrl MO) or (**B**) *tmem88a* (T88a MO) morpholino. Images on the right (insets) are higher magnifications of cardiac and cranial tissues in each embryo. All views are lateral, anterior to the left. In the main panels, blood flow is obvious in the *p53* mutant (arrow in A), but absent in the *tmem88a* morphant, with pericardial edema (arrowhead in B). Brain (br), heart (hrt) and blood (bl) are indicated and a translucent heart-string is evident in the *tmem88a* morphant. n>50 embryos analyzed per panel. Scale bar: 0.1 mm in insets.

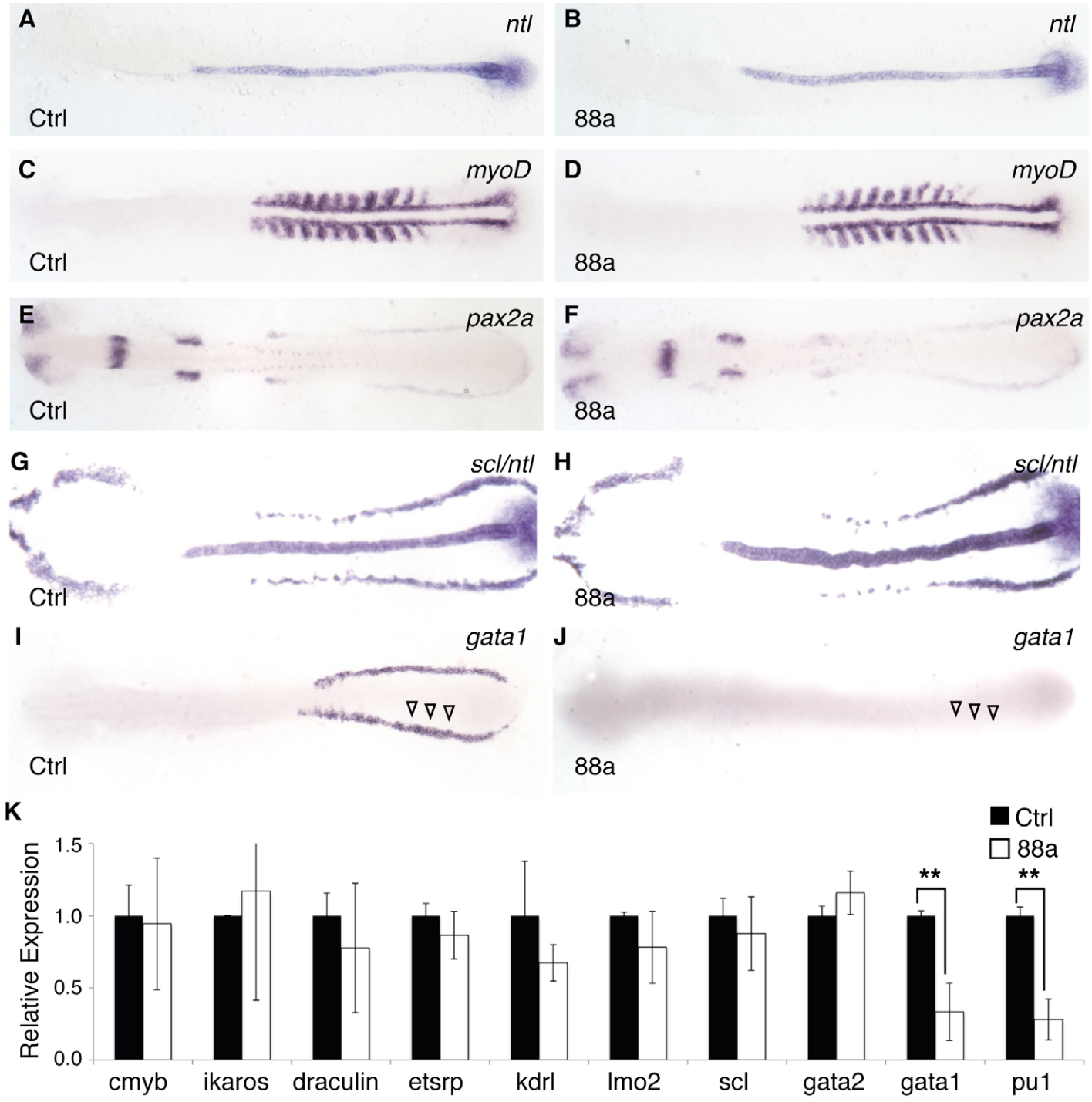

Fig. S8. Tmem88a depletion selectively affects lateral mesoderm derivatives including erythromyeloid progenitors. Flatmount preparations of representative 8- to 10-somite stage control (Ctrl) and *tmem88a* (88a) morphant embryos processed by WISH for (**A**,**B**) *ntl*$^{+}$ axial mesoderm, (**C**,**D**) *myod*+ paraxial mesoderm, (**E**,**F**) *pax2a*$^{+}$ intermediate mesoderm and (**G**,**H**) *scl*$^{+}$ hematovascular domains in the context of *ntl*. (**I**,**J**) *gata1*$^{+}$ hematopoietic progenitors. *n*>20 embryos per condition. (**K**) Relative expression levels by qPCR for various hematopoietic and vascular markers. ***P*<0.01.

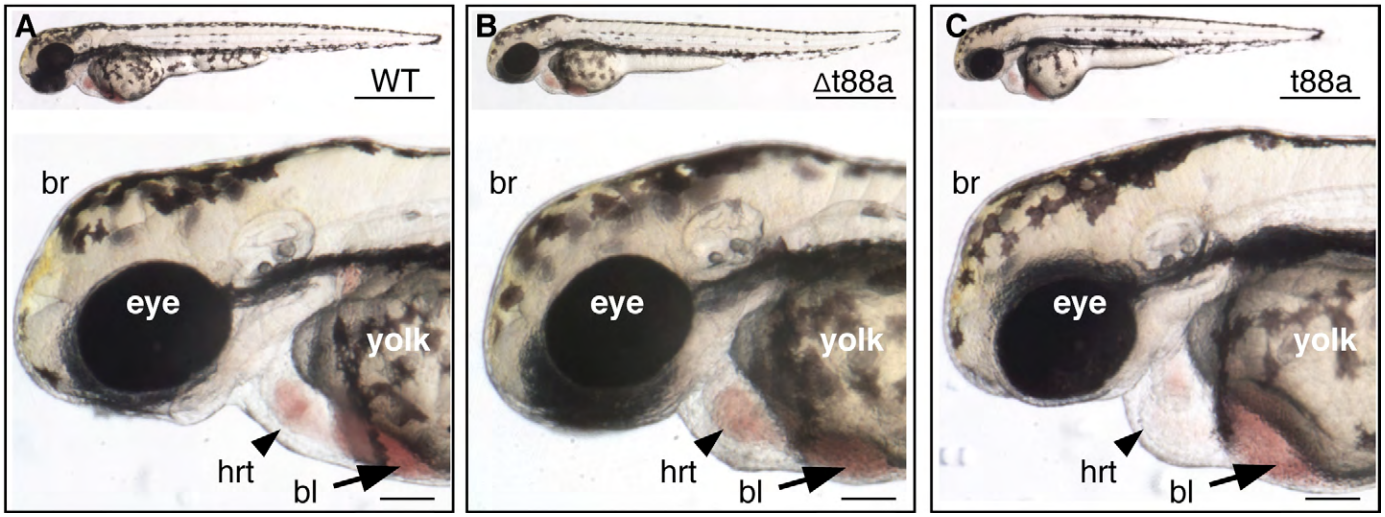

Fig. S9. Tmem88a overexpression causes cardiomyopathy. Brightfield images of 48-hpf (**A**) wild-type (WT) embryos, (**B**) embryos injected with mutated *tmem88a* mRNA (Δt88a) and (**C**) embryos injected with wild-type *tmem88a* mRNA (t88a). Brain (br), heart (hrt) and blood (bl) are indicated. *n*>50 embryos analyzed per panel. Scale bars: 0.5 mm (top) and 0.1 mm (bottom).

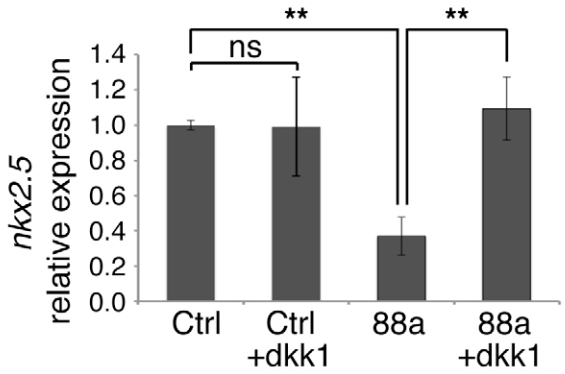

Fig. S10. Expression levels for *nkx2.5* are rescued in *tmem88a* morphants by WNT inhibition. *nkx2.5* relative expression levels by qPCR in control (Ctrl) and *tmem88a* morphants (88a) with or without WNT inhibition (+dkk1).

Table S1. Genes downregulated at least 2-fold specific to *gata5/6* double morphants at the bud and 6-somite stages.

Download Table S1